1-1-2021

APPLICATIONS OF HOT-MELT EXTRUSION (HME) TECHNOLOGY AND INVESTIGATION OF A SCREENING TOOL FOR HME

Gauri Deepak Shadambikar
University of Mississippi

APPLICATIONS OF HOT-MELT EXTRUSION (HME) TECHNOLOGY AND INVESTIGATION OF A SCREENING TOOL FOR HME

A Dissertation

Presented in partial fulfilment of requirements

For the Doctoral of Philosophy in Pharmaceutical Sciences with an emphasis in Pharmaceutics and Drug Delivery

The University of Mississippi

By

Gauri Shadambikar

August 2021

ABSTRACT

Hot-melt extrusion (HME), an adaptable technology, has established its position in manufacturing operations like amorphous solid dispersions, immediate and controlled oral formulations, implants and taste masked products. In recent years the industrial focus has shifted towards continuous manufacturing, thus HME is being explored for new applications. The aim of this research was to investigate the novel applications of HME by carrying out an in-depth study to understand the interaction between the process and product and to investigate a screening tool for its small-scale formulation and development.

As HME consumes large amount of samples during the developmental phase, we investigated a screening tool by using minimum quantity of active pharmaceutical ingredient. Vacuum Compression Molding (VCM) is a fusion based method to form solid specimens starting from powders. Mixtures of indomethacin with drug carriers were processed using VCM and HME. Thermal characterization such as differential scanning calorimetry and powder x-ray diffraction along with dissolution studies were performed to prove the effectiveness of VCM as a screening tool for HME based formulations at small scale.

The conventional techniques used for the preparation of nanostructured lipid carriers (NLC) are multi-step and time-consuming batch processes with low productivity. Hence, the continuous manufacturing advantage of HME was investigated for the preparation of NLC along with its process variation impact on the formulation composition. After optimization of screw configuration and process parameters, these formulations were successfully prepared using HME

in a continuous manner. In addition, the itraconazole NLCs were explored for the pulmonary drug delivery by characterizing its aerodynamic properties thereby showing promising results for pulmonary aspergillosis treatment.

To overcome the disadvantages associated with conventional liquid self-micro emulsifying drug delivery systems (SMEDDS), solid SMEDDS were formulated using HME. Solid surfactants were used to emulsify the lipids in the formulation. The prepared solid SMEDDS were characterized for globule size, PDI, zeta potential, dissolution test and differential scanning calorimetry. HME has gained attention in the pharmaceutical industry but its potential in preparing solid SMEDDS is still unexplored. Hence, solid SMEDDS were manufactured using HME for the first time.

DEDICATION

This work is dedicated to my family; Deepak Shadambikar and Anjali Shadambikar, my brother Vishwesh Shadambikar, Sushrut Marathe and all my mentors.

ACKNOWLEDGEMENT

My years at Ole Miss have been like a roller coaster ride of ups and downs. This journey was possible due to immense contribution from a number of people, for which I am forever grateful. I would like to express my deep and sincere gratitude to:

Dr. Michael A. Repka for his unwavering support, constant motivation and for being a strong pillar, no matter what challenges I encountered. He has always been my strongest advocate and source of encouragement to explore new ideas for which I am endlessly indebted. Dr. Soumyajit Majumdar for believing in me and providing scientific guidance and invaluable insights in my research endeavors.

Dr. Mahavir Chougule for giving me key inputs on my research work and thereby strengthening my dissertation work and project. Dr. Samir Ross for serving on my committee and for all his suggestions to improve my dissertation.

Ms. Deborah Herod for the constant help with all the paperwork right from my first day until this day. Dr. Suresh Bandari, for helping me in conducting research and writing manuscripts.

Dr. Finn Bauer, Dr. Thomas Kipping, Dr. Daniel Treffer and everyone else from Merck, Darmstadt, Germany for giving me an extraordinary opportunity of working with them. Sushrut, Pengchong, Peilun, Mashan, Nan Ji and other lab mates for helping relentlessly in the laboratory and for adding value to my research projects. Dr. Rohit Joshi and Supriya for always supporting and guiding me.

Table of Contents

List of Tables

List of Figures

CHAPTER I

INTRODUCTION TO HOT-MELT EXTRUSION

Nowadays, the percentage of new molecular entities with poor solubility is likely to increase with the development in combinatorial chemistry and significant importance of lipophilic receptors[1]. Thus, such compounds with poor water solubility present a major challenge during the drug development program, as dissolution of drug in the aqueous environment is the pre-requisite for absorption and distribution process[2]. The various approaches used for improving drug solubility include pH adjustment, co-crystals, co-solvents, surfactants, particle size reduction, amorphous solid dispersions, and lipid-based formulations[3]. Among these methods solid dispersions is a prominent technique to enhance the solubility[4]. Solid dispersion is a system in which one or more active ingredients are molecularly distributed into an inert carrier matrix[5].

Hot-melt extrusion (HME) technology was primarily developed for improving the solubility and bioavailability of poorly water-soluble drugs by preparing and manufacturing amorphous solid dispersions[6]. The process of HME was established in 1930s and it is widely used since then for rubber, plastic and food industry[2]. Since the last 20 years application of HME technology was expanded into the pharmaceutical industry for formulation and product development. HME is a continuous process that involves pumping of the polymeric materials with the rotating screws at temperatures above their glass transition or melting temperatures to

achieve molecular level mixing of the active compound and the polymer[7]. This molecular mixing converts the components into amorphous product thereby increasing the dissolution of the poorly water-soluble compound[2]. The extrusion equipment is classified into 3 main categories: ram, radial screen, and roll and screw extruders. Among these, the screw extruders are the most important because they continuously convert the fed material into the finished form such as rod or film[8]. Pharmaceutical extruder screws are designed based on the desired extrudates and modified as per the regulatory guidelines for the manufacture of the dosage form. They are classified as single, twin and multi screw extruder. Irrespective of the type of the screws are capable to rotate at the given operational speed. The screws are fixed inside the extrusion barrel that is heated to the desired temperature. HME is regarded as a green technology as it can be used for materials with high viscosity without any solvents. The technique is also amenable to continuous manufacturing and hence is an industrially feasible platform technology. Other advantages include shorter processing times, fewer unit operations, and relatively easy to scale up[9]. HME is a very flexible technology and there are numerous modifications that could be performed with the instrument to suit the formulator's needs. Currently, there are many FDA approved formulations commercially available such as Lacrisert, Kaletra, NuvaRing and Zythromax etc. Currently, research scientists are now investigating new applications of HME, to utilize this technique to its full potential. In recent years, it has been explored for the 3D-printing using the fused deposition modeling (FDM) printers[10].

CHAPTER II

VACUUM COMPRESSION MOLDING AS A SCREENING TOOL TO INVESTIGATE CARRIER SUITABILITY FOR HOT-MELT EXTRUSION FORMULATIONS

2.1. INTRODUCTION

In 1971, hot-melt extrusion (HME) was introduced as a formulation technology platform for the pharmaceutical industry[11]. Neither solvents nor complicated processing steps are required in HME to formulate a specialized drug delivery formulation. It can be used for the formulation of various drug delivery systems, but one of its significant uses is to improve the solubility of poorly soluble drugs[12]. This is one of the key challenges in today's research in formulation and development. Most of the new drugs under development have poor solubility of the active pharmaceutical ingredients[13]. The solubility and permeability of a drug are categorized by the biopharmaceutical classification system (BCS) into four classes based on its aqueous solubility and intestinal permeability[14]. The percentage of new molecular entities with poor solubility is likely to increase due to development in combinatorial chemistry and the significant importance of lipophilic receptors[1]. The creation of amorphous solid dispersions (ASD) is one way of formulating such poorly soluble drugs[15]. The solubility and bioavailability can be improved by orders of magnitudes via HME[16]. The solid-state of the poorly soluble crystals is changed via HME. They are dissolved within the polymer matrix when processed in the molten state. Once cooled down, the individual molecules are entrapped within the polymer matrix, forming a dispersed solid solution. When the solid solution is dissolved, the polymer matrix controls the dissolution rate and releases the individual molecules of the active substance. High supersaturation

levels can be maintained over a long time when suitable excipients are selected. Novel generations of amorphous solid dispersions are aiming to improve the dissolution profile of the carrier matrix by applying ingredients that provide additional surface activity or self-emulsifying properties[17]. Despite this advantage, it can also increase the risk of recrystallization during storage. Amphiphilic polymers can provide a relevant advantage, as no additional excipients are required to ensure the supersaturation of low soluble compounds.

Even with increasing demand, HME lacks reliable tools for formulation development, which allows access to reliable material data on a small scale. The HME technology was developed for processing plastics, and most of the development efforts were put on efficiency and maximizing the throughput[6]. When it was brought into the pharmaceutical labs, the smallest plastic extruders were adapted to suit the pharmaceutical manufacturing practices. To address the need to perform small scale screening, the equipment was downsized in dimensions or its concept slightly changed to reduce the minimum amount of material required to generate initial results[18]. Small scale extruders require at least a few grams of a material to allow first fusion-based investigations. The large fraction of the material however is lost during the startup phase or remains in the dead zone of the extruder. Formulation development with new chemical entities (NCEs) with this limitation is impractical as the available quantity of the Active Pharmaceutical Ingredient (API) is the limiting factor. Thus, to develop HME-based formulations comprising NCE, material sparing selection tools are necessary[19]. The HME technology is already quite established with several products like Lacrisert®, Kaletra®, Nucynta®, NuvaRing®, Zythromax® in the market[20].

1.1.1. Hot-melt Extrusion

Very few articles are published with the use of HME in first stage investigations. Some reports use a combined approach of hot stage microscopy and 5 mm twin-screw extruders in their

study to observe the change in crystal form and dissolution of the sample under the influence of the temperature for the development of scale up[19,21]. The development of implants by hot-melt extrusion necessitated the use of small-scale extruders with small batch sizes. For the predictive formulation of protein loaded implants, a 9-mm twin-screw extruder was used[22]. To determine operational and performance qualification on mixing in solid dispersion preparation in early-stage HME development, a conical twin-screw extruder was utilized[23].

1.1.2. Differential Scanning Calorimetry

Differential scanning calorimetry (DSC), an established analytical method, is one of the many thermal methods used as a screening tool to predict the drug-polymer solubility[24]. Experimental DSC data was used to predict a drug-polymer phase diagram and miscibility for Felodipine and polyacrylic acid[25]. Knopp et al. predicted drug-polymer solubility at elevated temperatures from DSC data for binary systems of five model drugs with PVP and PVA[24]. Similarly, for HME formulations, the solubility of crystalline drugs in the polymer was determined by a combined approach of DSC measurements and a reliable mathematical algorithm to determine a complete solubility of a drug in a polymer[26]. The solubility measurements for the compounds with very low absolute solubilities or exhibiting small changes in solubilities with temperature cannot give reliable results when analyzed by DSC[27].

1.1.3. Solvent casting

Solvent casting is usually applied to generate the first insights into a new API/carrier formulation. However, for a fusion-based product via HME, its results might deviate. A recent publication combines solvent casting with a simplified extrusion step to become a fusion-based screening method[28]. Novel approaches are also combining rapid solvent evaporation methods with an additional heating step, which is quite successful in estimating formulation performance[29]. To

utilize a minimum amount of drug, some research reports a high throughput screening technology developed by utilizing a 96 well plate system to identify optimal drug load and polymer using a solvent casting method[30].

One drawback of solvent casting is to find a common solvent where the polymers and drug substances together will be solubilized. Especially for hydrophilic polymers, this proves to be a challenge.

1.1.4. Vacuum Compression Molding

To overcome the above limitation of established screening tools, a novel approach to screen the new chemical entity with the polymer can be done using Vacuum Compression Molding (VCM). VCM is a fusion-based method to form solid specimens starting from powders. The process was first introduced in 2014 for sample preparation for rheological measurements of pharmaceutical polymers[31]. For the rheological measurement discs with 25 mm were introduced.

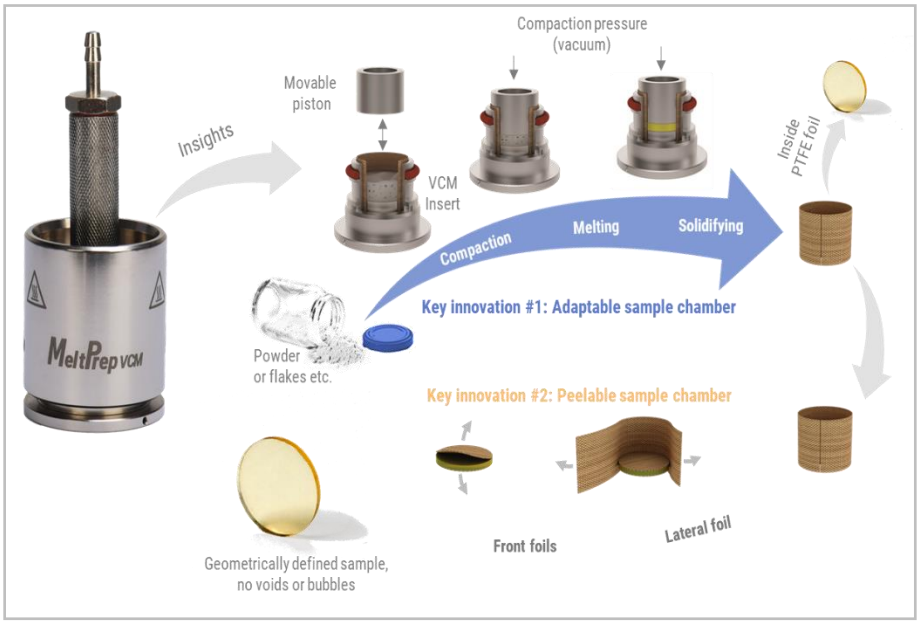

Figure 1-. MeltPrep® VCM Process.

The centerpiece of the VCM Process is the sample chamber. It is a chamber that is fully lined by PTFE foils and still adaptable in volume. The arrangement of three separation foils forms the PTFE

lining. One lateral foil covers the inner cylindrical surface of the VCM chamber, and two circular front foils cover the top and the bottom surface of the chamber. The starting material in powder form is filled inside the chamber formed by the foils. Once a vacuum is applied, the piston is pressed with 150N on the sample, which compacts the powder bed. The VCM Tool is subsequently placed on the hot plate of the VCM Essential to warm and then fuse the particles to a homogeneous sample. Since everything occurs under a vacuum within the tool, no air bubbles are entrapped within the polymer melt. The VCM Tool is quenched on the cooling unit by contact cooling and convection by a directed air cooling. The sample can be easily released from the chamber as the PTFE foils have excellent non-stick behavior and can be peeled off like a sticker from the sample. The method works without macroscopic mixing as only minimal mechanical mixing occurs during the processing when particles fuse. Larger particles in the millimeter and sub-millimeter range will not form homogeneous results. They require diffusion as the dominant mixing mechanism to obtain extrusion-like results. Hence, preconditioning of the powder before VCM processing is required when formulations with several components are molded to obtain homogeneous samples. The preconditioning can be obtained via cryogenic milling as it can alter the polymorphic structures[32].

The processing towards a solid form devoid of air inclusions was not possible in a lossless manner before the introduction of VCM. The VCM process has attracted the attention of several research groups and has been successfully applied to the screening of HME formulations like multilayer intravaginal rings[33]. Another group was speeding up the development of abuse-resistant formulations[34]. Evans et al. used VCM for material characterization to determine the solid density of API loaded formulations, which was subsequently fed into a 1d simulation software of extruders to predict processing behavior best possible[35]. Since VCM results in samples with a defined surface

area which corresponds to the cylinder surface, it enables intrinsic dissolution testing. It allows eliminating surface effects on the dissolution tests. The dissolution of polymer formulations is a complex topic and is described in several articles[36,37]. Insights can be obtained by dissolution measurements on samples with defined geometries. Dissolution mechanisms like surface erosion, bulk erosion, swelling, or diffusion behavior can be studied on quickly accessible VCM samples. Dissolution tests on the VCM samples enables direct performance comparison. Results can be used to tailor the particle size of a final dosage form. If powder or granules are required for the development when a conventional compacted tablet is desired, VCM samples of example 2-5 grams per batch can be milled afterwards and used for the development tasks.

The objective of the study was to investigate the VCM processability for ASD and to compare its results with HME processed formulations. Mixtures of Indomethacin (IND) with drug carriers (Parteck® MXP, Soluplus®, Kollidon® VA 64, Eudragit® EPO) were processed using VCM and extrusion technology. From the literature, it was found that indomethacin can form a stable ASD with Soluplus®, Kollidon® VA 64, and Eudragit® EPO. These excipients were able to enhance the solubility and inhibit crystallization for indomethacin. Until now, the interaction of Parteck® MXP and indomethacin has not yet been investigated. This paper gives insight into ASD using Parteck® MXP. The thermal characterization of the ASD was performed using differential scanning calorimetry and X-ray powder diffraction. The drug release performances were evaluated in simulated gastric fluid[38].

2.2. MATERIALS AND METHOD

2.2.1. Materials

Indomethacin was obtained from Sigma-Aldrich (St. Louis, MO, USA). Parteck® MXP was purchased from EMD Millipore Sigma (Darmstadt, Germany). Soluplus® and Kollidon® VA-

64 was purchased from BASF (Ludwigshafen, Germany). Eudragit® EPO was purchased from Evonik Industries (Essen, Germany). The marketed product (Indo-CT 50 mg capsules) was purchased from AbZ Pharma (Ulm, Germany). All other reagents were of either high-performance liquid chromatography (HPLC) or analytical grade.

2.2.2. Active Pharmaceutical Ingredient (API)

The model API used in this study was indomethacin (IND) which is a BCS class II compound. Its physicochemical properties are summarized in Table 1. Indomethacin is a potent Non-Steroidal Anti-Inflammatory drug[39]. It is poorly water-soluble with low glass transition temperature and thermally stable making it a good choice of model drug for amorphous solid dispersions[40].

Table 1. Physicochemical properties of model drug.

API	**M_w (g/mol)**	**logP**	**T_m (°C)**	**T_g (°C)**	**pKa**	**SGF Solubility**[41]
Indomethacin	357.8	4.27	155 ±0.1	49 ±0.1	4.5	0.004g/1000g

2.2.3. Carriers

The excipients selected for the present study were Kollidon®-VA64 a copovidone-(vinylpyrrolidone-vinyl-acetate), Soluplus® a graft copolymer (polyvinyl-caprolactam-polyvinyl-acetate-polyethylene-glycol), Parteck® MXP (polyvinyl-alcohol), and Eudragit® EPO (poly-methyl-methacrylate). The physicochemical properties of the excipients are mentioned in the Table 2.

Table 2. Physicochemical properties of polymers used in ASD

Polymer	**Classification**	**Average Molecular Weight (g/mol)**	**Glass Transition (°C)**	**Degradation Temperature (°C)**	**Water Solubility (pH-7)**
Parteck®MXP[42]	Non-ionic	32,000	54	250	Soluble

Soluplus® [43]	Non-ionic	118,000	65-70	250	Soluble
Kollidon®VA-64[43]	Non-ionic	45,000	100	230	Soluble
Eudragit® EPO[44]	Ionic	47,000	48	200	Insoluble

2.2.4. Marketed Drug Product for Reference

Indo-CT 50 mg capsules were used as a reference in the release study. They are 50 mg hard capsules with indomethacin as the active ingredient. It is used for symptomatic treatment of pain and inflammation.

2.3. Processing Methods

2.2.5. Preparation of Cryo-milled Mixtures for VCM Preparation- Preconditioning of the samples.

Polymer – Indomethacin (30% w/w) binary mixtures were weighed and then mixed in Turbula® Mixer (Willy A. Bachofen AG, Switzerland) for 5 minutes. The mixture was then cryo-milled with liquid nitrogen in Ultra-Centrifugal Mill ZM-200 (Retsch GmbH, Germany) at 18000 rpm and sieved through a mesh size of 250 µm.

2.2.6. Vacuum Compression Molding (VCM)

The MeltPrep® VCM Tool consisted of a sample holder, piston, and lid. The sticking of the sample during the preparation was prevented using separation foils. The sample holder was connected to a vacuum source. The cryo-milled mixture was filled into the sample holder which provided amorphous samples of 8 mm & 20 mm in diameter. The 8mm discs were intended to provide intrinsic like dissolution, and the 20 mm discs were further processed via milling to create enough material to allow a direct comparison between milled extrudate and milled VCM material. The piston provided the pressure on the sample, which was heated on the hot plate till a homogenous mixture was obtained. The heating process was followed by rapid cooling to get the final product. Table 3 summarizes the parameters from MeltPrep® samples with 20 mm and 8 mm

in diameter. Target temperatures and respective heating times were adapted and optimized for the individual polymers.

Table 3. Processing parameter of VCM samples.

Polymers	20mm VCM Disc Insert		8mm VCM Disc Insert	
	Heating Temperature (°C)	Heating Time (min)	Heating Temperature (°C)	Heating Time (min)
Parteck® MXP	230	5	230	5
Soluplus®	170	5	170	4
Kollidon® VA-64	160	5	160	4
Eudragit® EPO	190	5	190	4

Samples produced via VCM have a defined geometry and yield transparent glasslike discs once amorphous systems are obtained. The circular cross-section for 25 mm discs, as it was initially introduced, is 490 mm^2 so that for materials with densities of around 1 g/cm^3; 1 gram is enough to obtain a solid disc with around 2 mm height. The VCM process has attracted the attention of several pharmaceutical research groups quickly as it offers extrusion-like results, and the required material amount is comparatively lower to the existing extrusion methods.

The amounts can be drastically reduced further by simply reducing the disc dimensions to smaller diameters, as it will be shown during the study. This small disc's diameter (e.g., 2 or 5 mm) enables sample preparation of small quantities starting in ranges from 10 mg and in addition to that, an opportunity to meet similar material demands compared to solvent casting methods.

2.2.7. Hot-melt Extrusion (HME)

For the extrusion process, the pre-blended physical drug-polymer mixture was fed into the hopper. Each of these resultant drug-polymer binary mixtures containing 30% w/w of the drug was extruded utilizing an 11 mm co-rotating Pharma twin-screw extruder and Congrav twin-screw feeder (Thermo Fisher Scientific®, Waltham, MA, USA) equipped with a 2-mm round opening die. Differential scanning calorimetry was utilized to determine the extrusion processing

temperature range. The target temperature for extrusion was above the melting point of indomethacin. For Soluplus®, Kollidon® VA 64 and Eudragit® EPO was at about 160℃, anticipating the additional heat impact due to shear forces. For Parteck® MXP the temperature profile needed to be increased to overcome the polymer's semi-crystalline alignment. Hence the extrusion temperature was set at 190℃. A standard screw configuration consisting of conveying and kneading elements was used (Figure 2) at a screw speed of 200 RPM. A constant feed rate of 0.2 kg/h was employed for all formulations. The process parameters were recorded, and the conditions of the steady-state operation are given in Table 4.

Table 4. HME Process Parameters.

Polymer	**Pressure (bar)**	**Melt temperature (°C)**	**Barrel Temperature for all the zones (°C)**	**Torque % of max.**	**Torque (Nm)**
Parteck® MXP	8-10	181	190	20	1-2
Soluplus®	1	151	160	24	1-4
Kollidon® VA 64	0-1	152	160	40	2-4
Eudragit® EPO	0	152	160	43	2-6

Figure 2. Screw configuration for Thermo Fisher Scientific® Pharma 11-mm extrusion.

2.4. Characterization Methods

2.3.1. Physical characterization of the VCM samples

The VCM samples were characterized for the uniformity of weight using a Mettler Toledo® analytical balance. The before and after sample weights were statistically assessed via a two-tailed

paired t-test (IBM® SPSS® Statistics 25). The significance threshold was set at a p-value of 0.05. The samples were visually inspected for transparency, potential recrystallization, and bubbles.

2.3.2. Differential Scanning Calorimetry (DSC)

The thermal properties of the polymer excipients, API, and samples prepared in the present study were investigated using a DSC 3+ differential scanning calorimeter (Mettler-Toledo®, Greifensee, Switzerland). Nitrogen was used as the purge gas at a flow rate of 50 ml/min. For sample analysis, 5-7 mg samples were accurately weighed and sealed inside aluminum pans. The lids were pierced by the autosampler before the measurement was initiated. For thermal characterization, pure indomethacin, and the milled VCM and HME materials were heated at 10 °C/min from 25 to 300 °C. Results were analyzed using STARe SW 16.00 software.

2.3.3. PXRD Analysis

PXRD patterns were recorded on a Stoe StadiP® 611 instruments (Stoe, Germany) equipped with a Cu radiation source (λ = 1.54 Å) and a Mythen1K Si-strip detector. Measurements were conducted in transmission and at an acceleration voltage of 40 kV and a current of 40 mA. Scanning was performed over an angle range of 2θ at a step size of 0.015° and dwell time of 0.5s. The results were analyzed using Powdat software.

2.3.4. Dissolution

The dissolution tests were carried out for the marketed product and indomethacin loaded samples prepared using VCM and HME. Prior to the test, the 20 mm VCM and HME samples were milled. An equivalent of 50 mg of indomethacin milled samples were used for dissolution. The 8 mm VCM discs which were equivalent to 50 mg of indomethacin were used as an entire disc. The marketed formulation (Indo-CT 50 mg) was used as a reference. The dissolution tests were carried out using the Sotax AT7 smart (Sotax, Germany) dissolution tester following the USP

apparatus 2 method. The dissolution medium was 900 ml of simulated gastric fluid (SGF) at 37.5 ± 0.5 °C with a stirring rate of 75 rpm. SGF was selected as a dissolution media to determine solubility of indomethacin in stomach on oral administration. Three replicates were performed for each sample. The amount of indomethacin dissolved was determined using the online UV-VIS method at 318 nm.

2.5. RESULTS AND DISCUSSION

2.4.1. Vacuum Compression Molding

Images of the produced VCM discs are shown in Figure 3. The VCM discs had a defined cylindrical geometry and a yellowish appearance with all polymers. All discs were transparent, no crystals were visible, indicating that indomethacin was dissolved in the carrier materials. The Kollidon®VA64 samples occasionally showed some bubbles, which might be related to residual moisture of the material. Compared to extrusion temperature readings, VCM requires slightly higher hot plate temperatures to compensate for non-existing shear heating. It does not mean that VCM requires higher processing temperatures compared to the macroscopic extruder temperature readings, as the readouts of the extruder do not capture local shear heating within the polymer melt. Temperature increases of 20°C or even more are typical values obtained by simulations conducted to evaluate shear heating during twin-screw extrusion[45]. Table 5 shows the lossless preparation of the VCM samples produced for a filling weight of 167 and 500 mg for 8 mm and 20 mm, respectively. The resulting VCM samples were showing that no material was lost during VCM processing. This was statistically analyzed by comparing before and after weights for each corresponding polymer mixtures with a two-tailed paired t-test with a confidence interval of 95%. A *p*-value of more than 0.05 was obtained for each of the comparisons indicating that the difference is non-significant. The visual inspection indicated amorphization, and the samples were further

analyzed in the subsequent analysis sections. The VCM samples (n=3 for each dimension) as used to screen one formulation required less than 2 grams of starting material, which corresponds to 1/5 of the 3-minute flushing time of the small-scale extruder chosen for this study. Further, potential downscaling using small-scale analysis tools will also allow using smaller VCM tools, e.g., with 2 mm diameter, making screenings in the mg-scale feasible.

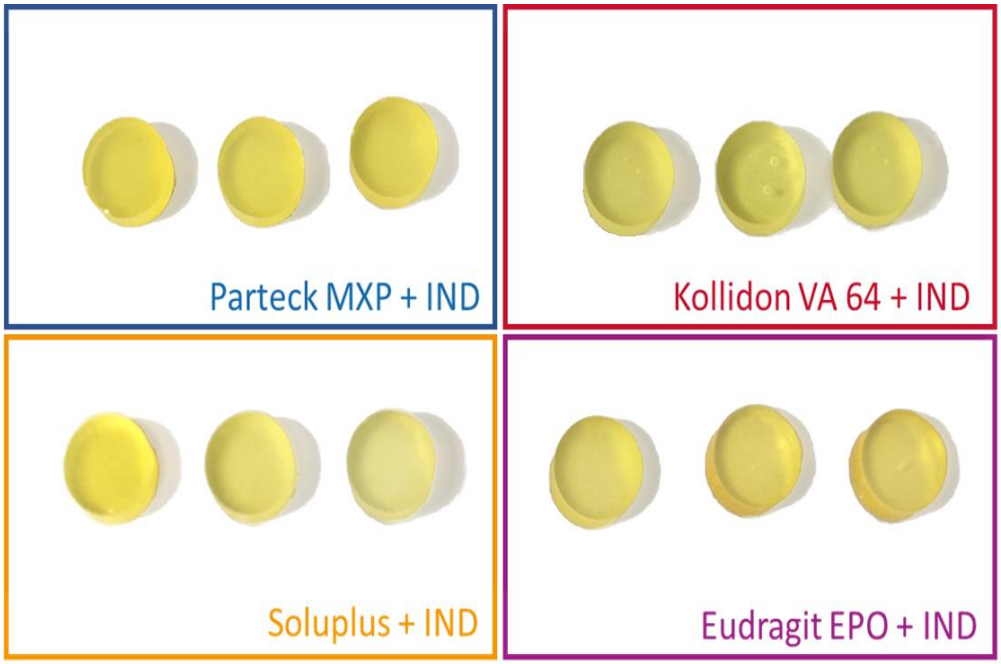

Figure 3. Images of 8 mm VCM Disc Samples loaded with 30% IND (20 mm diameter not shown, similar in appearance).

Table 5. Lossless Preparation of MeltPrep® VCM Samples (n=3).

Excipients	**Before VCM Process Weight (mg)**		**After VCM Process Weight (mg)**	
	8 mm	**20 mm**	**8 mm**	**20 mm**
Parteck® MXP	167.51 ± 0.29	498.35 ± 0.84	166.46 ± 0.39	495.75 ± 1.77
Soluplus®	168.67 ± 1.21	502.43 ± 1.27	166.90 ± 0.56	499.20 ± 0.31
Kollidon® VA 64	167.23 ± 2.05	500.85 ± 1.57	165.47 ± 2.56	498.98 ± 1.68
Eudragit® EPO	167.24 ± 1.78	500.12 0.45	165.37 ± 1.08	497.39 ± 1.32

2.4.2. Hot-melt Extrusion

The extrusion was started under the parameters mentioned in 2.2.7. HME. All evaluated polymers were processed at the identified parameters. The obtained extrudates were pelletized using a Brabender strand pelletizer (Brabender GmbH & Co. KG, Duisburg, Germany) with a pellet size of 2mm and further milled for all the evaluations (IKA tube mill 100, Staufen, Germany) to provide a similar particle size compared to the material used for a fast disintegration tablet. All the polymers utilized showed good extrudability under the utilized processing temperatures.

2.4.3. Differential Scanning Calorimetry

Thermal analytical techniques provide data about thermal stability, melting point, and recrystallization temperatures[38]. The sharp endothermic peak at 162 °C corresponds to the melting point of indomethacin (Figure 4). Parteck® MXP, Soluplus®, Kollidon® VA64, and Eudragit® EPO showed T_g (glass transition) temperatures of 50 °C, 70 °C, 101 °C and 57 °C respectively, confirming their amorphous state (Figure 4 left). An endothermic melting peak at 180 °C was observed for the Parteck® MXP indicating its semi-crystalline nature caused by an alignment of the linear polymer chains.

Indomethacin was completely miscible at the concentration of 30% w/w in the polymer-carriers, which is an important prerequisite to attain a solid dispersion. A characteristic melting endothermic indomethacin peak was absent in the VCM and HME formulations (Figure 4 middle and right). Thus, it confirmed that the indomethacin was present in an amorphous state in the VCM discs and melt-extruded formulations. The semi-crystalline peak for Parteck® MXP is still observed in the VCM formulations proving its semi-crystalline nature which is unaffected by the VCM and HME processing.

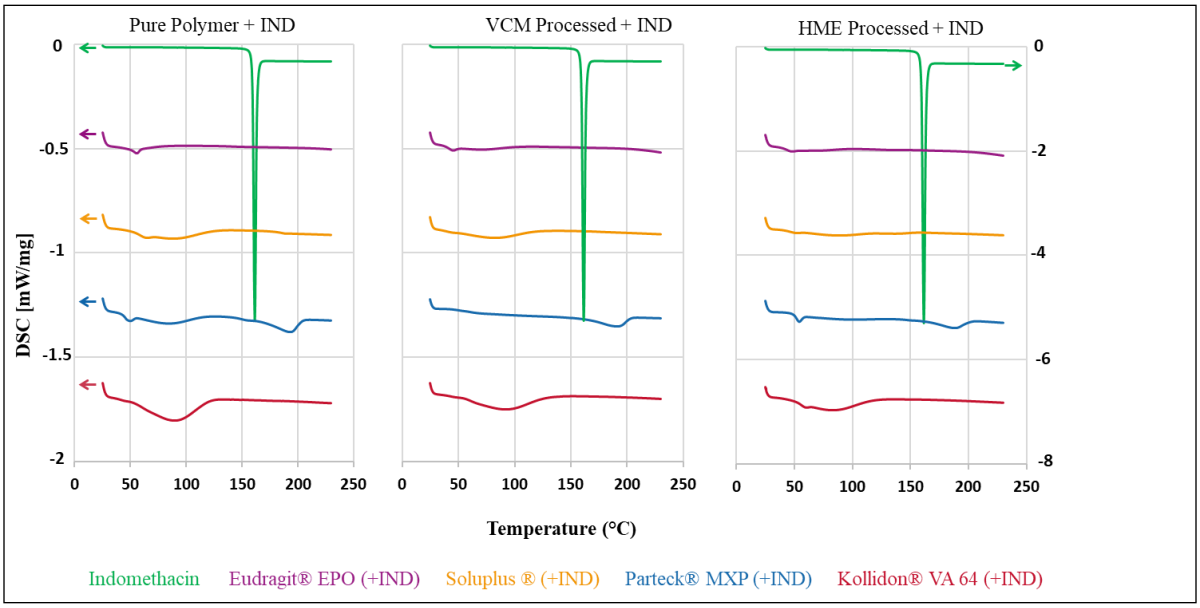

Figure 4. DSC thermogram left: neat polymers and IND; middle: milled VCM material from processed mixtures of polymers and IND (20mm); right: milled HME material from processed mixtures of polymers and IND; heat flow offset used for better visibility.

2.4.4. PXRD Analysis

DSC studies indicated drug-polymer miscibility in the HME and VCM formulations. However, DSC measurements have limited sensitivity of measuring crystalline residuals within the material. Therefore, the solid-state of the formulations were further investigated by the PXRD analysis.

Figure 5 shows the diffractograms of the measured data of processed VCM samples as well as the cryo-milled physical mixtures of each polymer and indomethacin. Figure 6 shows the diffractograms of processed HME samples. The reference data of pure indomethacin shows a significant crystalline peak confirming the crystalline state of the starting material.

XRD pattern for the milled extrudate and milled VCM samples showed a complete absence of characteristic crystalline peaks of indomethacin. Both melt processing routes (HME and VCM)

deliver comparable results. In contrast, Parteck® MXP shows a broad halo between 2θ of 19°–25° confirming the semi-crystalline nature of PVA polymer.

The solid-state of the cryo-milled mixtures, as seen in Figure 5, is already influenced via the cryo-milling process. The effect of cryo-milling on polymorphic transformation has been reported earlier for indomethacin[46]. The formation of an amorphous state upon cryo-milling is because of the continuous disordering process of the indomethacin lattice. This observed amorphization in indomethacin is a cryo-milling time-dependent process, and it has been extensively studied and reported[47,48]. In the case of Parteck® MXP and Kollidon® VA 64, this effect is seen to be more pronounced than in Eudragit® EPO and Soluplus®. As cryo-milling was not the objective of the study, the observed differences in the amorphization of the physical mixtures were not further explored.

When VCM screening is applied, cryo-milling is beneficial since it provides uniform mixing and size reduction for the physical mixture. The short cryo-milling as preconditioning decreases the physical mixtures crystallinity by bringing the path length (particle dimensions) down to small length scales that can make diffusion as the main mixing mechanism. The VCM process can achieve the full amorphization of the subjected formulation without stressing the material.

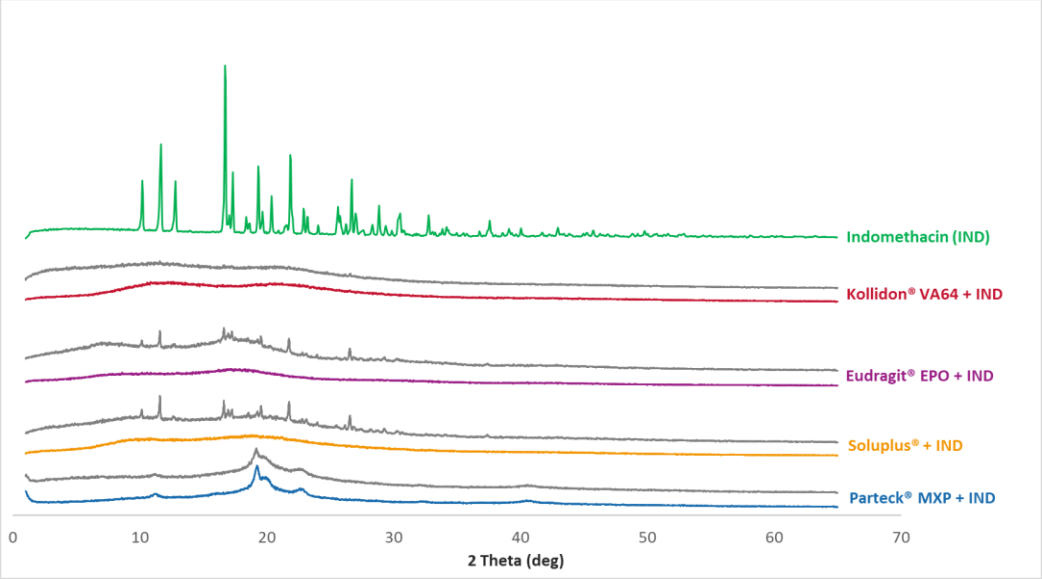

Figure 5. PXRD Measurements: The curves for the formulations are clustered. In front of each cluster is the VCM processed samples with color code used throughout the data; and in the back is the cryo-milled physical mixtures for each polymer and indomethacin dep

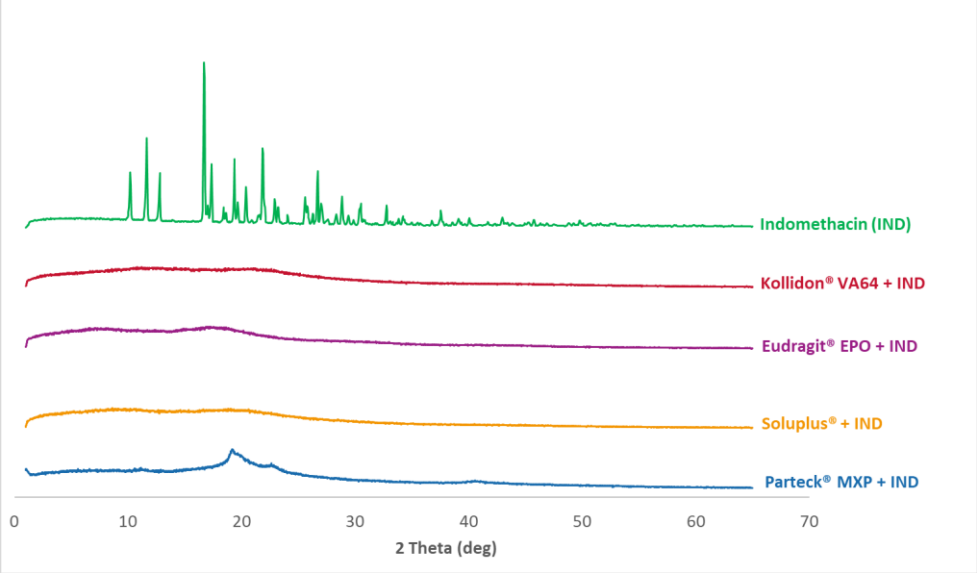

Figure 6. PXRD Measurements: Diffractograms for processed HME samples and pure indomethacin diffractogram for reference purpose is given in the back as a single curve.

2.4.5. Dissolution

Dissolution data of milled VCM samples and milled HME samples are presented in Figure 7 and Figure 8, respectively. Figure 9 represents the dissolution data of the entire 8 mm VCM discs. Simulated gastric fluid (pH 1.2) was chosen to evaluate the supersaturation of indomethacin via the amorphous matrix. The 8 mm discs were directly used for the dissolution while the 20 mm samples were milled. The factors that played a vital role in the release behavior were the nature of the excipients and the surface area of the samples during the dissolution study. In the case of 8 mm discs, as they were placed intact in the dissolution medium, it had less surface area and hence very small surface was exposed to the dissolution medium to facilitate the drug release. While the 20 mm VCM and HME samples were milled, a large surface area was available for drug dissolution.

The similarity between the milled VCM and HME samples is shown using the *f2* similarity value. As per the FDA guidelines, the release profiles are considered similar when the *f2* value is greater than 50. If more than 85% of the drug is released, only a single value above that is considered[49]. But in the case of our results, the steady-state concentration for all the formulations was found to be less than 85%. Hence, for the *f2* value calculations, we considered all the timepoints from the study.

A very rapid onset can be observed for Eudragit® EPO in the milled VCM and HME samples with a release of 45.04 ± 0.19 mg/L in 10 minutes and 46.00 ± 0.88 mg/L in 15 minutes, respectively. After an initial supersaturation for Eudragit® EPO, precipitation occurs resulting in reduced concentrations. After 60 minutes, Eudragit® EPO was able to maintain the drug concentration of at least 4.68 ± 0.20 mg/L for milled VCM samples and 6.53 ± 0.05 mg/L for milled HME samples till the end of the study. The observed release is due to the pH-sensitive solubility of Eudragit® EPO in gastric juices up to a pH of 5.0[50]. From the similarity factor (*f2*

value) the drug release profile for milled VCM and HME samples is similar with the *f2* value of 50.79 (Table 6).

For the Eudragit® EPO 8 mm VCM discs, the highest concentration of 35.63 ± 2.21 mg/L was reached in 25 minutes. Similar to, the milled samples, after an initial supersaturation a stable plateau was observed at 105 minutes with a drug concentration of 6.88 ± 0.38 mg/L. The 8 mm VCM disc was completely dissolved by 360 minutes (Figure 10) as Eudragit® EPO is highly soluble in pH 1.2, which correlates with an initial burst release.

Parteck® MXP showed a peak drug concentration of 20.17 ± 0.70 mg/L at 120 minutes for milled VCM samples and then maintained a minimum drug concentration of more than 20.10 ± 0.98 mg/L till the end of 360 minutes. In the case of milled HME samples, the peak drug concentration of 23.02 ± 0.22 mg/L was observed at 60 minutes, and a drug concentration of more than 17.99 ± 0.29 mg/L was maintained. In contrast to Eudragit® EPO, it can maintain the supersaturation for a longer timeframe. Due to its surface-active properties, polyvinyl alcohol of Parteck® MXP can effectively stabilize the supersaturated state for a prolonged timeframe[51].

For the Parteck® MXP 8 mm VCM discs, a sustained and incomplete release is observed with 17.28 ± 0.53 mg/L in 360 minutes owing to the diffusion behavior from the intact matrix of the disc. In the case of Parteck® MXP milled HME samples and milled VCM samples had an *f2* value of 70.33, showing that the drug release profiles are similar.

In all the Kollidon® VA 64 formulations, a supersaturation is observed but with limited drug release during the entire release period. With the highest drug release of 9.29 ± 0.47 mg/L for milled VCM samples, 7.40 ± 1.92 mg/L for milled HME samples, and 6.58 ± 0.79 mg/L for 8 mm VCM discs at 360 minutes. The observed results can be explained as Kollidon® VA 64 at a pH of 1.2, may preferentially dissolve from the matrix's exterior by forming a drug-rich amorphous

hydrophobic shell that inhibits the drug release[52]. As seen from Figure 10, the 8 mm VCM disc had retained its shape and did not show any disintegration for the drug release to occur. For the milled VCM and HME samples, an *f2* value of 84.59 was calculated, thus proving a similar release pattern.

Unlike the other excipients, extremely limited release from the Soluplus® was observed. In the milled VCM samples, a release of 12.25 ± 0.69 mg/L, and for milled HME samples a release of 3.44 ± 0.5 mg/L was observed at 360 minutes. The *f2* value of 61.19 was obtained, proving a similar release behavior. For, the 8 mm VCM discs the negligible release was observed with a maximum release of 0.28 ± 0.05 mg/L. From Figure 10, we can see that Soluplus® shows water absorption and swelling while retaining the disc-like shape. The limited release from Soluplus® can be attributed to the possible formation of hydrogen bonds between the carboxylic groups on indomethacin and oxygen atoms in the Soluplus®. Due to the formation of hydrogen bonding at pH 1.2, there is a reduction in the solubility of the polymer leading to decreased release[53]. Also, in the case of an 8 mm VCM disc, the surface area available for drug release is limited, while in the case of milled samples, the surface area is increased multi-folds. This increase in the surface area can explain the observed higher drug release from milled samples despite low solubility.

Compared to other polymers, PVA shows at least 4 times higher drug release than Soluplus®, Kollidon® VA 64, and the marketed formulation Indo-CT 50 mg. Furthermore, compared to the solubility of the pure indomethacin, Parteck® MXP enhanced the release by almost 20 times.

The area under the curve (AUC) was calculated using the trapezoidal rule for the release profiles of milled HME, milled VCM, 8mm VCM disc, and the marketed product Indo-CT 50 mg (Table 7). Considering the obtained AUC results of milled VCM, milled HME, and 8mm discs,

we can establish an overall ranking of the polymers for ASD. From all the polymers, Parteck® MXP showed the highest maintained supersaturation levels for indomethacin in the case of milled as well as 8mm disc samples. It was followed by Eudragit® EPO, Kollidon® VA64, and then Soluplus®. The high variability of AUCs observed for Soluplus®, can be attributed to the factors mentioned above like available surface area and hydrogen bonding. Collectively, if we compare the results obtained via the VCM tool to the results of the hot-melt extruded formulations in Figures 7 and 8 a remarkably similar pattern can be observed. This highlights the high predictability of the MeltPrep® VCM technology. The performance of different polymers can be assessed at a low sample size and provide high reliability of prediction.

Table 6. Similarity factor (f2) for the VCM 20 mm samples and HME samples.

Polymer	***f2* value**
Parteck® MXP	70.33
Soluplus®	61.19
Kollidon® VA 64	84.59
Eudragit® EPO	51.78

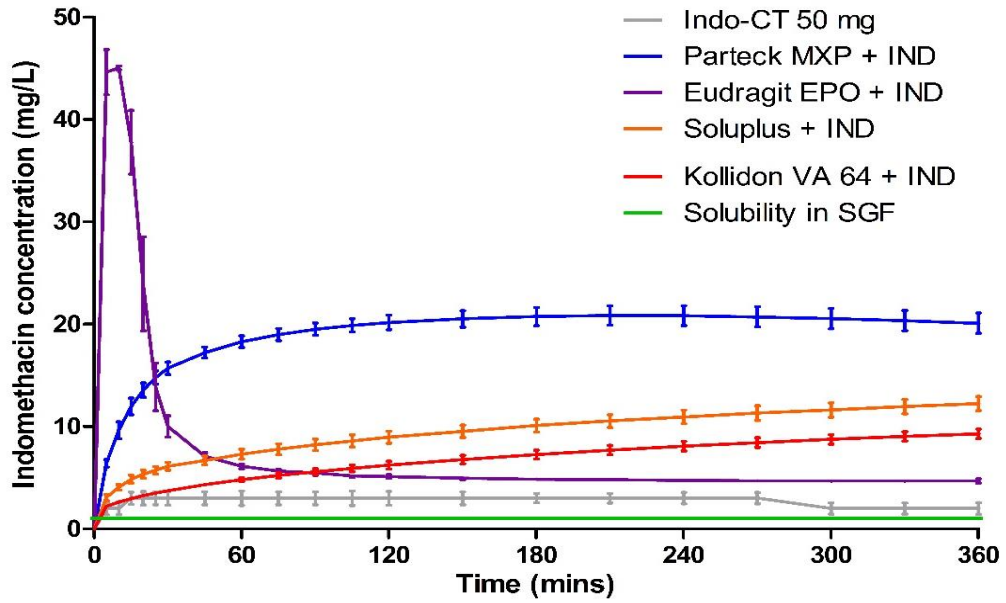

Figure 7. Dissolution testing for milled VCM material in Simulated Gastric Fluid.

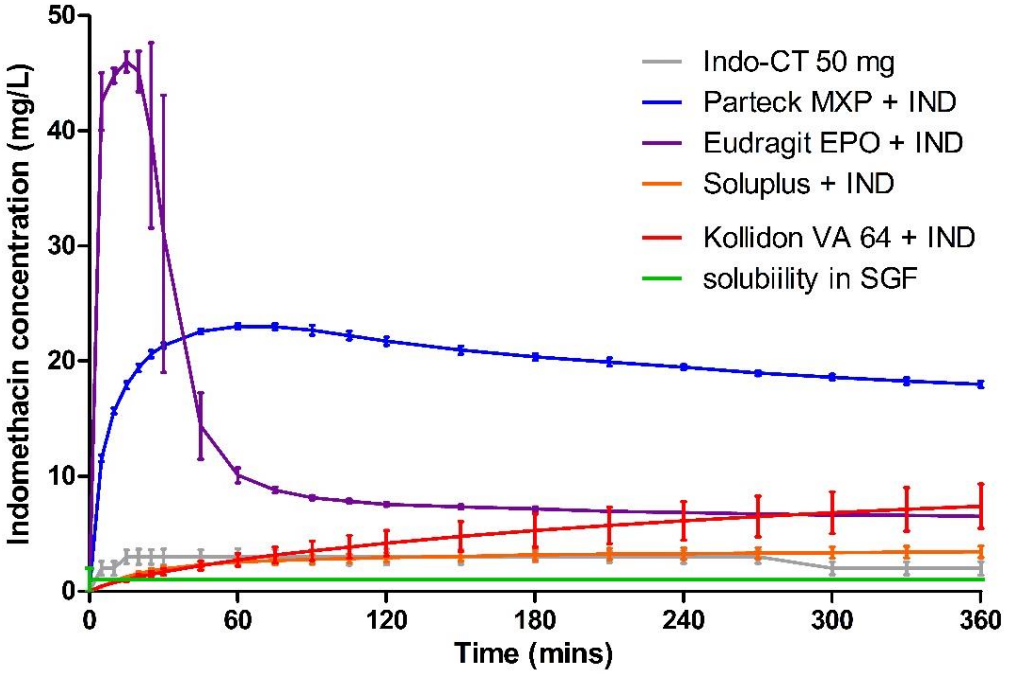

Figure 8. Dissolution testing for milled HME material in Simulated Gastric Fluid

Table 7. Area under the curve (AUC) ± RSD for release profiles of HME and VCM samples (n=3).

Polymer	Milled HME ($mg \cdot L^{-1} \cdot min$)	Milled VCM ($mg \cdot L^{-1} \cdot min$)	8 mm VCM ($mg \cdot L^{-1} \cdot min$)
Parteck® MXP	7196.02 ± 1.09	6940.29 ± 3.96	3778.45 ± 1.25
Soluplus®	1053.25 ± 14.22	3421.46 ± 7.52	57.31 ± 22.96
Kollidon® VA 64	1752.93 ± 25.91	2459.68 ± 6.43	1725.85 ± 14.17
Eudragit® EPO	3855.90 ± 5.74	2557.37 ± 2.38	3140.94 ± 7.94
Marketed Product - Indo-CT 50 mg – 933.33 ± 20.86 $mg \cdot L^{-1}min$			

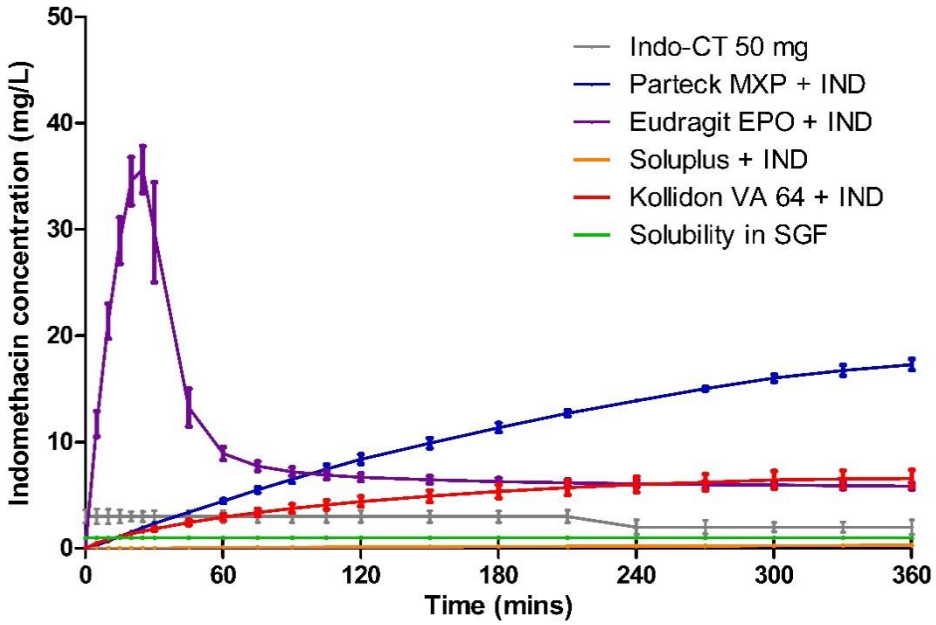

Figure 9. Dissolution testing for 8 mm VCM discs in Simulated Gastric Fluid.

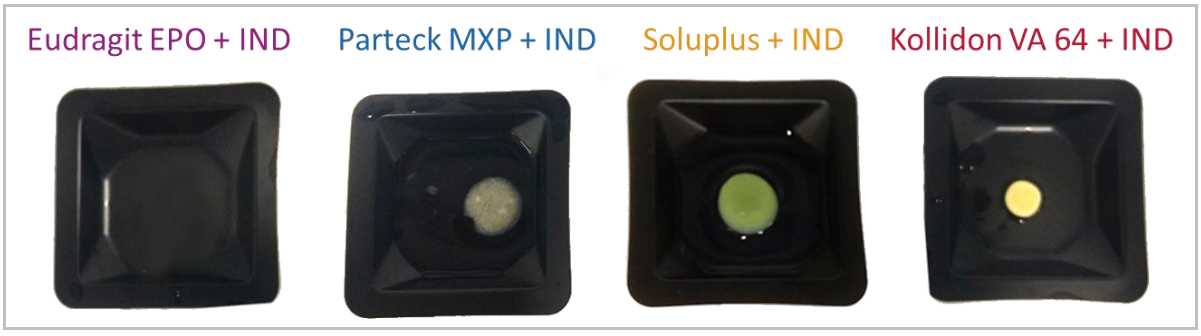

Figure 10. VCM Discs after 6 hours of dissolution on weighing boats

2.6. CONCLUSION

In this study, the MeltPrep® VCM technology was assessed as a potential screening tool for melt-based formulations at a small scale, where we also demonstrated the loss-less processing.

Indomethacin as a model drug was utilized for the preparation of solid dispersions using HME and VCM technology. The primary objective of the study was to compare the formation of ASDs to enhance the solubility of indomethacin and to assess the similarity between the two technologies. It was determined through the comparison of thermal analysis, PXRD, and dissolution profiles. From the DSC thermograms and PXRD diffractograms, we confirmed that an amorphous solid dispersion was formed using both the technologies. This was further proved by similar dissolution profiles indicating the comparability of the VCM samples to that of the HME. Hence, proving our objective of utilizing VCM as an explorative tool for HME based formulations. With fast preparation time, small sample amount requirements, and with choice of different sample sizes and shapes, VCM will be a feasible predictive tool for extruded formulations, especially on a small scale.

We could demonstrate the application of VCM technology for a set of widely used polymers in HME, especially showing a clear advantage for hydrophilic polymers, which would be potentially excluded by a standard film casting screening. Further processing of VCM samples such as milling can mimic particle properties as they would be obtained from milled extrudates enabling down-streaming to a conventional tablet design.

When comparing the efficiency, Parteck® MXP showed better results among all selected polymers. It was able to show a sustained drug release as well as maintained a steady-state concentration at a much higher level compared to other polymers. Even though Eudragit® EPO showed an initial burst release, the drug concentration quickly dropped down and was sustained at

a very low value compared to initial supersaturation concentration. While Soluplus® and Kollidon® VA 64 showed a drug release of less than 20% in 360 minutes.

One advantage of the early screening technology is to identify potential interactions between drug substances and test polymers at early development stages like the observed low drug release in the case of Soluplus®. VCM utilizes small quantities of material compared to HME, thus preventing the wastage of material in early development screening.

A visual analysis of the samples during the dissolution process can provide important insight into the release mechanism. Understanding molecular interactions within the matrix can support the identification of the best possible carrier at the early stages.

CHAPTER III

FORMULATION DEVELOPMENT OF INHALABLE ITRACONAZOLE LOADED PEGYLATED NANO-LIPID CARRIERS USING HOT-MELT EXTRUSION TECHNOLOGY

3.1. INTRODUCTION

Inhalation drug delivery is a potential route for the treatment of various pulmonary disorders. It has several advantages as compared to the conventional oral or parenteral route[54]. It reduces frequent dosing, avoids first pass metabolism, the inhaled drug directly reaches the lung epithelium and it is noninvasive[55]. The lung has large surface area for absorption (~100 m^2) and thin absorption membrane (0.1 – 0.2 µm)[56]. In last few years, there has been an increasing interest in the pulmonary route of drug delivery due to the potential use of lung as a portal for localized therapeutic agent and systemic delivery. In inhalation drug delivery, the usage of biodegradable nanoparticles has proved to be advantageous to attain the extended release of loaded drug while protecting the drug from degradation[57]. Nano lipid carriers (NLC) are matrix based particle formulated using solid state lipid and liquid state lipids which confers them higher drug loading and stability than the solid lipid nanoparticles which comprise of solid state lipids[58]. NLCs are complex structures which are surrounded by outer solid shell while the inner core comprises of oil and this allows for a higher drug load of lipophilic drugs[59]. They have been investigated for various drug delivery routes such as oral, topical and ocular etc.

Pulmonary Aspergillosis is an opportunistic fungal disease that occurs in the immunocompromised patients[60]. Even with the development of new diagnosis and therapies, the

overall mortality rate remains approximately 50%[61]. It is already proven that nebulization of antifungal drugs to the lungs enhance the therapy by achieving high, localized concentration while avoiding systemic toxicity when compared with oral route of administration[62].

Itraconazole (ITZ) is a poorly water-soluble, BCS class II, antifungal drug which is widely used to treat various fungal infections such as Aspergillosis[63]. It has an n-octanol/water partition coefficient of 5.66 at pH 8.1[64]. The oral ITZ capsule has box warning of congestive heart failure and drug interaction. ITZ is known to cause hepatotoxicity, cardiac dysrhythmias, peripheral neuropathy, and hearing loss and hence it use is limited[65]. The inhalation delivery of ITZ at lower dose will overcome these limitations associated with oral delivery.

During the disease state the pulmonary airways are covered with a layer of mucus which is particularly viscoelastic and difficult to penetrate[66]. It has been demonstrated that drug loaded nanoparticles with 2K PEG coating with dense-brush border coating (10 mole %) achieved the mucus penetration of nanoparticles[67-68]. PEG is a hydrophilic, nonionic and nontoxic polymer[69]. It is an effective steric stabilizer due to its hydrophilicity, electrical neutrality and chain flexibility[70]. The mucus clearance and macrophage are two main mechanisms responsible for clearance in the lungs. The use of PEG on the surface of nanoparticles, provides hydrophilic corona and neutral charge on the surface which will reduce the macrophage uptake[71]. Thus, providing the increase in the lung residence time. In addition, the PEG coating provides salt and serum stability. The property of PEG coating on nanoparticles helps in shielding the surface from aggregation and minimize the phagocytosis and opsonization which is well established[72].

High pressure homogenization (HPH), micro emulsification and solvent displacement are some of the current methods used in preparation of NLCs[73]. However, these methods involve

multistep processing such as melting of lipids, dispersion of drug in the molten lipids, addition of aqueous phase, mixing and then size reduction hence making it a batch process[74]. Methods such as solvent displacement entails disadvantages such as use of organic solvents which further needs removal to prevent toxicity. HPH has been explored for its feasibility in scale up and is most preferred method for the preparation of nanoparticles[75]. However, it is considered as a method with long processing time and batch to batch variations[9]. In the pharmaceutical industry, a continuous manufacturing is preferred over a batch process as it reduces the cost of production, labor and resources. The conventional methods have a risk of batch-to-batch variations that lead to variable product outcomes of the NLCs such as particle size, polydispersion indices and entrapment efficiency of the drug. In comparison a continuous process it can provide higher efficiency and improved product quality attributes[76].

Hot melt extrusion technology (HME) is a continuous process of pumping raw materials at high temperatures and pressure to get a uniform product[77]. This process offers many advantages over the conventional pharmaceutical manufacturing processes. Since it eliminates the use of solvent it provides environmental advantages along with the shorter and efficient processing time to formulate the final product[78,15]. Hence, HME has emerged as an innovative technology to produce pharmaceutical dosage forms such as tablets, capsules, implants, and films over the traditional techniques[79].

The hypothesis of this investigation was to develop and evaluate the continuous and scalable itraconazole PEGylated nano-lipid carriers of <250 nm using hot melt extrusion coupled with probe sonication for inhalation delivery. The main objective of this study was to investigate the formulation strategy based on the HME technology in the preparation of the inhalable PEGylated itraconazole loaded NLCs (ITZ-PEG-NLC) and while doing so, the process parameters

were optimized to formulate a product with good quality attributes. Furthermore, the ITZ-PEG-NLC were investigated for the inhalation drug delivery of itraconazole by examining the effects of ITZ-PEG-NLC on the release of itraconazole, aerodynamic properties, and *in vitro* cytotoxicity against the A549 cells.

3.2. MATERIALS AND METHODS

3.2.1. Materials

Itraconazole was obtained from TCI Chemicals (Portland, OR), N-(carbonyl-methoxypolyethyleneglycol-2000)-1,2-distearoyl-sn-glycero-3-phosphoethanolamine sodium salt (mPEG-2K-DSPE sodium salt) was purchased from Lipoid (Ludwigshafen, Germany). Precirol ATO 5 was a generous gift from Gattefossé (Paramus, NJ). Tween 80, Oleic acid were purchased from Acros Organics (Morris, NJ).

3.2.2. Method

3.2.3. Preliminary Study

Lipids were selected based on the literature data for the solubility of ITZ. It showed good solubility in solid lipid Precirol ATO 5 and liquid lipid Oleic acid[64]. Polysorbate 80 was selected as surfactant for its good emulsifying and stabilizing properties. The drug concentration of ITZ was found to be a critical parameter in the stability of the NLCs due to its inherently low solubility in the lipids. Higher concentrations of ITZ showed solubilization issues and induced precipitation on preparation of formulations. The process parameters such as the screw speed and screw configuration of HME and sonication time were considered to have an effect on the formulation characteristics.

3.2.4. Differential Scanning Calorimetry (DSC)

A differential scanning calorimeter (DSC 25, TA instruments, New Castle, DS, USA) was employed to observe the melting and the recrystallization behavior of the drug with the excipients and to determine the barrel temperature for the hot-melt extruder. Approximately 5 mg of the samples, individually sealed in the aluminum pans were placed over the sample platform. The samples included ITZ, precirol ATO 5, PEG-2K-DSPE and the physical mixture. The reference pan, empty sealed aluminum pan was placed on the reference platform. The pans were heated from 25 to 200 °C at the rate of 10 °C/min under nitrogen purge (50 mL/min).

3.2.5. Preparation of PEG-ITZ-NLC Formulation

A schematic illustration of ITZ-PEG-NLC formulation by HME-Probe Sonication system is shown in Figure 11. For the preparation of ITZ-PEG-NLC using HME (11 mm Process 11, ThermoFisher® Scientific, Karlsruhe, Germany) a modified screw configuration (Figure 12) was used so that with increase in mixing elements, the ITZ and the lipids are properly exposed to the surfactant solution and mixed efficiently to obtain a pre-emulsion. The preparation involved 2 steps. The first step was to prepare the formulation by pumping all the raw materials into the barrel and the second step was to reduce the size by probe sonication to formulate the NLCs. The volumetric feeder and the peristaltic pumps were calibrated depending on the ratio of solid physical mixture to liquid lipid and aqueous solution. The composition of the formulation was kept constants for all the NLCs (Table 8).

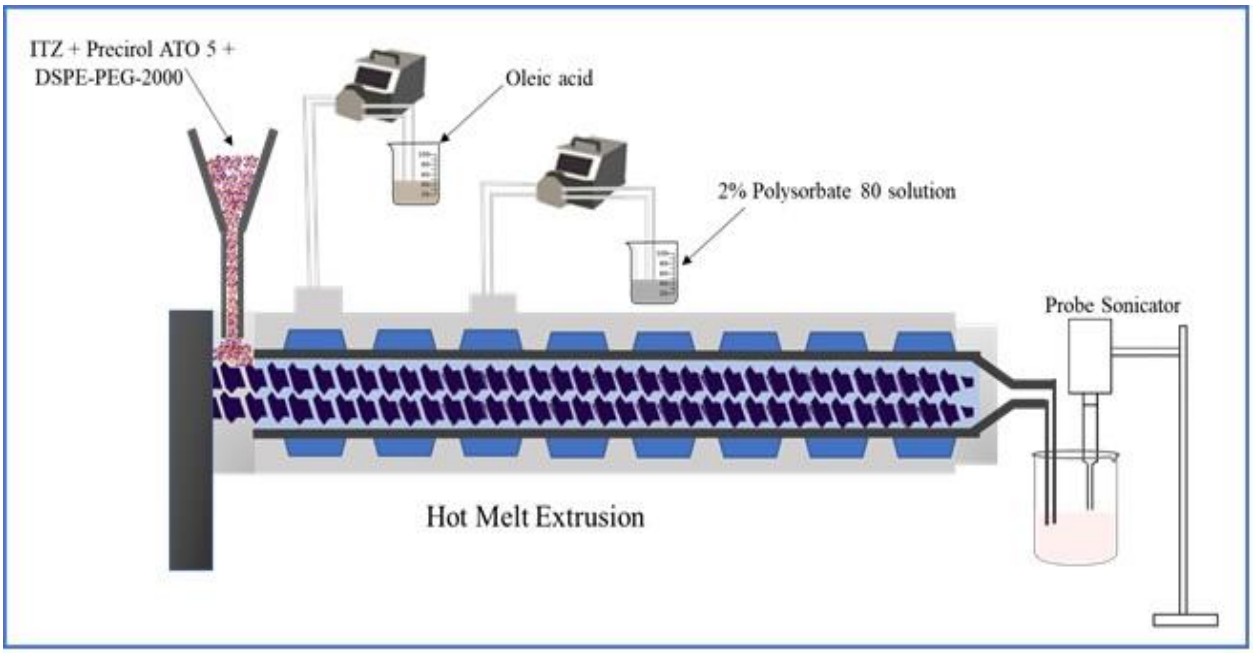

Figure 11. Schematic illustration for the preparation of ITZ-PEG-NLC using hot melt extrusion along with probe sonication

The ITZ was uniformly mixed with the Precirol ATO 5 and PEG-2K-DSPE using a V-shell blender (Maxiblend®, GlobePharma, New Brunswick, NJ, USA) and introduced into the barrel using a volumetric feeder. The oleic acid and aqueous solution equivalent to the extrusion temperature were added into the barrel using a peristaltic pump in the zone 2 and zone 4 respectively. The introduction of aqueous solution in the barrel should begin after the mixture of lipids reach zone 4. The barrel temperature for the zone 1 and zone 2 was 120 °C and the remaining zones had a temperature of 85 °C. The three screw speeds of 50, 100, 150 rpm were used in the study to determine their influence on the product. The obtained hot pre-emulsion was then probe sonicated (Vibra-Cell Processor, Sonic and Material Inc., CT, USA) with 40% amplitude and pulse of 10 on 5 off for size reduction. The sonication time varied from 5, 10 and 15 minutes to check

the effect of sonication time on the particle size of ITZ-PEG-NLC. The formulations were stored at 25℃ for a period of 30 days for further characterization.

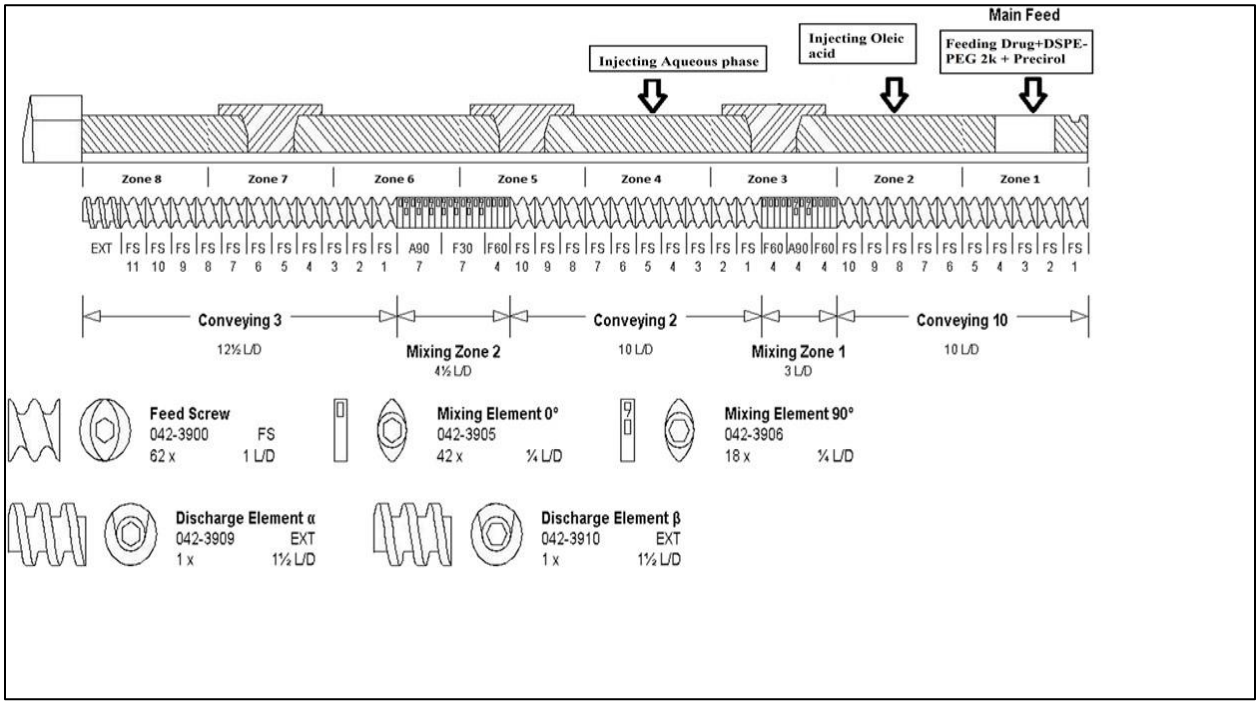

Figure 12. Modified screw configuration utilized in preparation of ITZ-PEG-NLC

Table 8. Composition of ITZ-PEG-NLC formulation.

Material	**Amount (%w/v)**
Itraconazole	0.025
Precirol ATO 5	5.4
Oleic acid	0.6
PEG-2K-DSPE	1
Polysorbate 80	2
Water	QS 100 mL

3.3. CHARACTERIZATION

3.3.1. Particle size, Polydispersity Index and Zeta Potential Analysis

The particle size, polydispersity index and zeta potential of the ITZ-PEG-NLC formulations were determined by photon correlation spectroscopy using a Zetasizer Nano ZS Zen3600 (Malvern® Instruments, Malvern, UK) at 25°C and with 173° backscatter detection in disposable folded capillary clear cells. The measurements were obtained using a helium neon laser, and the particle size analyses data were evaluated based on the volume distribution. Briefly, 10 µL of the sample was diluted to 1000 µL using the deionized water and the particle size and PDI were measured.

3.3.2. Entrapment Efficiency

The entrapment efficiency was determined by calculating the entrapped drug after removal of unentrapped drug using an Amicon® centrifugal filter (MWCO 10 kDa) units centrifuged at 13,000 rpm for 15 minutes. The filtrate was analyzed using the HPLC method described below. The following formula was used to calculate the % entrapment efficiency (EE):

$$\%EE = \frac{Amount\ of\ ITZ\ added - \ Amount\ of\ ITZ\ in\ filtrate}{Amount\ of\ ITZ\ added} \times 100$$

3.3.3. Assay (ITZ Content)

An accurately measured amount of ITZ-PEG-NLC (50 µL) was added into 5 ml volumetric flask with addition of 200 µL of dichloromethane (DCM) and dimethylsulfoxide (DMSO) in the ratio of (4:1) and the volume was made up to the mark with acetonitrile. The sample was centrifuged at 13000 rpm for 15 minutes and the supernatant was analyzed for the assay by HPLC.

3.3.4. In vitro release study

The *in vitro* release studies were conducted on day 0 and day 30 with a 10 ml of an aqueous solution containing 20% (w/v) 2-hydroxypropyl-beta cyclodextrin as a dissolution medium in scintillation glass vials maintained at 35 ± 0.5°C with magnetic stirring rate of 200 rpm. A separate scintillation glass vial with medium and formulation was utilized for each timepoint. To the medium of each scintillation glass vial, 1 mL of the ITZ-PEG-NLC formulation was added. For every time point, 400 µL of the sample was collected from the respective scintillation glass vial. The sample was centrifuged using 10kDa Amicon® filter for 15 min at 13,000 rpm and the permeant was analyzed by the HPLC for ITZ released into the medium. The experiments were performed in triplicate. The *in vitro* release method was adopted and modified as reported in literature. To compare the release profiles of the initial and stability samples, a similarity factor (f_2) was calculated. The equation of the similarity factor is represented in the equation below-

$$f2 = 50 \times \log\left\{\left[1 + (1/n)\sum_{t=1}^{n}\left(R_{t-T_t}\right)^2\right]^{-0.5} \times 100\right\}$$

Where R_t and T_t are % dissolved for the initial sample and stability sample, respectively at each time point while n denotes the number of time points. If the f2 value of the two release profiles is between 50 and 100, the initial and stable samples are considered similar.

3.3.5. HPLC method

The quantification of Itraconazole was performed using a Waters HPLC system with a Waters 2489 UV detector utilizing a Lune C18, 250 x 4.6 mm (5µ) Phenomenex column. The stock solution was prepared in mixture of DCM:DMSO in the ratio 4:1[80]. The mobile phase composed of a mixture of Acetonitrile and 0.1% aqueous solution of glacial acetic acid in the ratio

of 80:20. The UV spectrum was recorded at 267 nm with a flow rate of 1mL/min and injection volume of 20 µL.

3.3.6. Viscosity

The viscosity of ITZ-PEG-NLC was measured using a Brookfield cone and plate viscometer (LV-DV-II+ Pro Viscometer, Middleboro, MA, USA). Around 1 mL of the formulation was placed in the cup plate after adjusting the gap between the cone and plate. The formulation in the cup was maintained at 25 °C using a circulating water bath. A CPE 44 spindle was operated at varied speeds from 1 to 50 rpm and the viscosity was recorded from Rheocalc software.

3.3.7. Powder X-ray diffraction analysis

A qualitative powder X-ray diffraction (PXRD) was done (performed at the University of Texas, Austin) to examine the physical state of ITZ in the formulated ITZ-PEG-NLC. The X-ray powder diffraction patterns of the samples were recorded with the Rigaku X-ray system (D/MAX-2500PC, Rigaku Corp., Tokyo, Japan) using Cu rays (λ = 1.54056 Å) with a voltage of 40 kV and a current of 40 mA, over a 2θ scanning range of 5°–50°, with a step width of 0.02°/s and a scan speed of 0.02 s.

3.3.8. Nebulization of the PEG-ITZ-NLC

To observe the effect of nebulization on the particle size and PDI, the ITZ-PEG-NLC were nebulized using Philips Respironic Sami the Seal Nebulizer Compressor. For the study, 5 mL of the formulation was nebulized. The particle size and PDI of before nebulization formulation was measured. Then the formulation was nebulized, and the aerosol obtained was collected and analyzed (n=3).

3.3.9. *In vitro* aerosol characterization

Aerodynamic particle size distribution was measured using an 8 stage non-viable Anderson cascade impactor (ACI) (Westech® Scientific Instruments, UK). To prevent particle bounce and efficient particle capture during the nebulization, each plate on the impactor was coated with Polysorbate 80. The ITZ-PEG-NLC formulation was nebulized for 10 minutes into the cascade impactor operated at a flow rate of 28.3 L/min. After nebulization with the Philips Respironics Sami the Seal Nebulizer Compressor, the amount of formulation deposited on the impactor stages (0-7) and filter was collected and the amount of ITZ was analyzed using HPLC. Formulations were tested in triplicate and the fine particle fraction (FPF), mass median aerodynamic diameter (MMAD) and geometric standard deviation (GSD) were calculated.

3.3.10. *In vitro* cell viability

The cytotoxicity of PEG-IT-NLC was evaluated in the human adenocarcinoma alveolar basal epithelial A549 cell line. For comparison the PEG-Placebo was prepared for the cell viability studies. The A549 cells were seeded in 96 well micro titer plates at a density of 5000 cells/well and after overnight incubation the cells were treated with various concentrations of PEG-Placebo and ITZ-PEG-NLC diluted in the cell growth medium. The cells were cultured in HyClone™ Dulbecco's modified Eagle medium and maintained at 37°C with 5% CO_2 in a humidifier incubator. The cells were incubated for 24, 48 and 72 hours. The cell viability in each treatment at regular time intervals was determined using crystal violet assay. The relative cell number was calculated as the ratio of the absorbance of the treated well versus that of the untreated control. The obtained results were analyzed by one way ANOVA.

3.3.11. Morphological Characteristics using Tandem Electron Microscopy

A 20 uL drop of sample was placed on a sheet of clean parafilm. A freshly glow discharged 200 mesh copper grids coated with thin carbon film was floated film side down on the drop of NLC formulation. After 30 s, the grid was removed from the drop and the excess sample was removed by touching a piece of filter paper to the edge of the grid. Before complete drying the grids were placed sample size down on a drop of ultrapure water and immediately removed. Excess water was removed, and the grid sample side down was placed on a drop of 1% Uranyl acetate. Images were generated on a JEOL JEM-1400 Flash TEM and captured on Gatan One View digital camera.

3.3.12. Statistical Analysis

Statistical analysis was conducted using one-way ANOVA and two-way Repeated measures ANOVA (JASP 0.13.1.0). It was deemed as significant difference at $p < 0.05$.

3.4. RESULTS AND DISCUSSION

3.4.1. Formulation of ITZ-PEG-NLC

Process parameters such as screw speed of the HME and the sonication time were optimized for the formulation of the ITZ-PEG-NLC. The screw design, zone of liquid addition, drug and lipid concentration for the ITZ-PEG-NLC were optimized from the preliminary trials. The preliminary trials indicated that a modified screw design with a mixing element after zone 1 and 2 was efficient in mixing of oil with the solid lipid and ITZ. Further the next mixing element after addition of the aqueous phase provided efficient mixing of all the components in the barrel before ejection of the product from the barrel. The zone of liquid addition for the aqueous solution was determined based on the screw configuration and was optimized to be zone 4 compared to zone 3. The barrel temperature for all of the zones was optimized based on the thermal analysis of

the physical mixture. The zone 1 temperature was higher than the rest of the barrel to facilitate efficient melting and mixing of itraconazole within the components. In NLC preparation, the formation of the pre-emulsion is of utmost importance to achieve a stable formulation. The sonication time of the hot pre-emulsion influenced the size reduction and stability of the formulation. For all the HME runs, the feeding rate and torque were controlled to prevent formulation variations. The torque value obtained was less than 5% for all runs.

3.4.2. Differential Scanning Calorimetry

Differential Scanning Calorimeter was used for analyzing the melting and recrystallization behavior of the drug within the lipid phase and is shown in Fig 13. The melting point of ITZ is reported to be between 166 and 170°C[81] . A melting endothermic depression can be spotted at ~169 °C. The physical mixture of the drug in the lipid phase indicates a melting peak of the lipids at ~70 °C, coinciding with the melting point of Precirol ATO 5. The drug-lipid mixture thermograms did not show any endothermic peak for ITZ, suggesting either complete solubility of the drug in the lipid phase or conversion of the drug from crystalline to amorphous form.

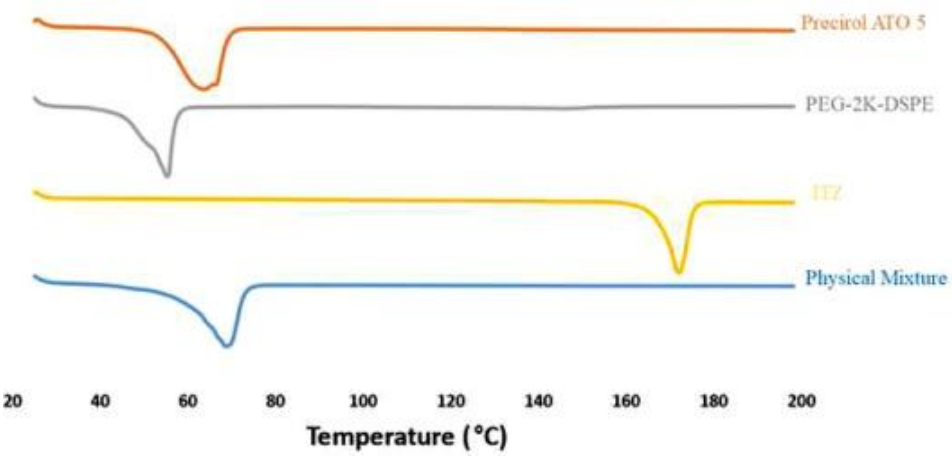

Figure 13. Differential scanning calorimetry thermograms.

3.4.3. Particle size, Polydispersity Index and Zeta Potential Analysis of NLC

Table 9. Particle size, PDI, Zeta Potential of ITZ-PEG-NLC Formulations for Day 0 and Day 30

Formulation No.	**Screw Speed (rpm)**	**Sonication time (mins)**	**Day 0**			**Day 30**		
			Particle size (nm)	**PDI**	**Zeta Potential (mV)**	**Particle size (nm)**	**PDI**	**Zeta Potential (mV)**
			Day 0			**Day 30**		
F 1	50	5	172.70 ± 14.66	0.24 ± 0.03	-24.80 ± 5.49	178.60 ± 10.04	0.39 ± 0.04	-21.60 ± 0.45
F 2	50	10	101.20 ± 1.69	0.26 ± 0.01	-19.10 ± 5.84	99.61 ± 1.33	0.22 ± 0.03	-15.60 ± 2.22
F 3	50	15	79.11 ± 1.66	0.20 ± 0.04	-23.60 ± 3.76	142.90 ± 6.75	0.37 ± 0.07	-16.80 ± 0.52
F 4	100	5	114.90 ± 4.09	0.34 ± 0.06	-26.30 ± 1.19	200.40 ± 6.24	0.05 ± 0.03	-18.60 ± 0.17
F 5	100	10	84.95 ± 1.19	0.22 ± 0.02	-20.20 ± 2.29	134.80 ± 0.36	0.17 ± 0.03	-16.80 ± 0.57
F 6	100	15	87.54 ± 1.60	0.24 ± 0.03	-22.50 ± 6.34	168.5 ± 9.20	0.38 ± 0.09	-17.40 ± 1.35
F 7	150	5	99.92 ± 0.89	0.22 ± 0.05	-28.90 ± 4.56	185.90 ± 29.06	0.22 ± 0.06	-19.20 ± 1.52
F 8	150	10	103.80 ± 2.72	0.281 ± 0.02	-20.30 ± 1.69	193.00 ± 3.08	0.22 ± 0.06	-18.20 ± 0.55
F 9	150	15	107.60 ± 1.79	0.372 ± 0.06	-20.50 ± 1.14	207.90 ± 7.17	0.27 ± 0.03	-16.70 ± 0.5

In the nebulization process the particle size is an important factor. To achieve enhanced delivery of the drug to the deep lungs, the particle size needs to be smaller due to diffusional mobility so that more number of nanoparticles will be accommodated into the micron size

droplet[82]. The table 9 represents the particle size, PDI and zeta potential of the 9 formulations on day 0 and day 30.

In NLC formulations, it is important to observe the storage stability rather than the particle size and PDI on day of preparation as the physiochemical characteristics of the NLCs can change during storage period. Hence, a one-way repeated measures ANOVA was conducted on particle size, PDI and zeta potential of the ITZ-PEG-NLC to evaluate the effects of the screw speed (***rpm***), sonication time (***mins***) on storage ***stability*** (***stability***). Assumptions of normality and sphericity were met due to the balanced nature of the design. The within subject effects in the repeated measured ANOVA describe the effects of the independent variables on the same sample measured at different time-points. These effects are seen as an interaction of the independent variables with the time dependent variable, in this case, storage ***stability***. So, in the analysis, the effect of the screw speed (***rpm***) and the sonication time (***mins***) on the particle size, PDI and zeta potential on storage is described as the interaction between storage ***stability*** and screw speed (***stability*rpm***), storage ***stability*** and sonication time (***stability*mins***) and storage ***stability***, screw speed and sonication time (***stability*rpm*mins***). The between subject effects explain the effects of the process variables (screw speed and sonication time) on different samples at different levels of independent variables. And they can be used to understand direct effect of screw speed and ***rpm*** on particle size, PDI and zeta potential of nanoparticles.

Table 10. Within subject effects of the variables

	Particle size	**PDI**	**Zeta Potential**
	p	***p***	***p***
Stability	0.011	0.902	<.001
Stability*rpm	.001	<.001	0.818
Stability*min	<.001	<.001	0.055
Stability*rpm*mins	0.269	<.001	0.135

Table 11. Within subject effects on the parameters

	Particle size	**PDI**	**Zeta Potential**
	p	***p***	***p***
Rpm	<.001	0.040	0.941
Mins	<.001	0.011	0.002
Rpm*mins	<.001	0.132	0.734

From the within subject effects, for the particle size analysis, the ***stability*rpm*** and ***stability*mins*** interactions were significant ($p < 0.001$) indicating the significant difference between particle size measured on day 1 and day 30 of the formulations with different screw speeds and sonication times (Figure 14a). In case of the PDI, the ***stability*rpm*mins*** interaction was significant ($p < 0.001$) indicating the significant effect of screw speed, sonication time and storage stability on difference between the PDI on Day 1 and Day 30 (Figure 14b). While in case of zeta potential, the ***rpm*** and sonication time ***(mins)*** did not affect the difference in zeta potential observed for the formulations on Day 1 and same formulations measured on day 30 (Figure 14c, $p>0.05$)). The observed result was the factor of the storage stability on the changes in zeta potential ($p < 0.001$).

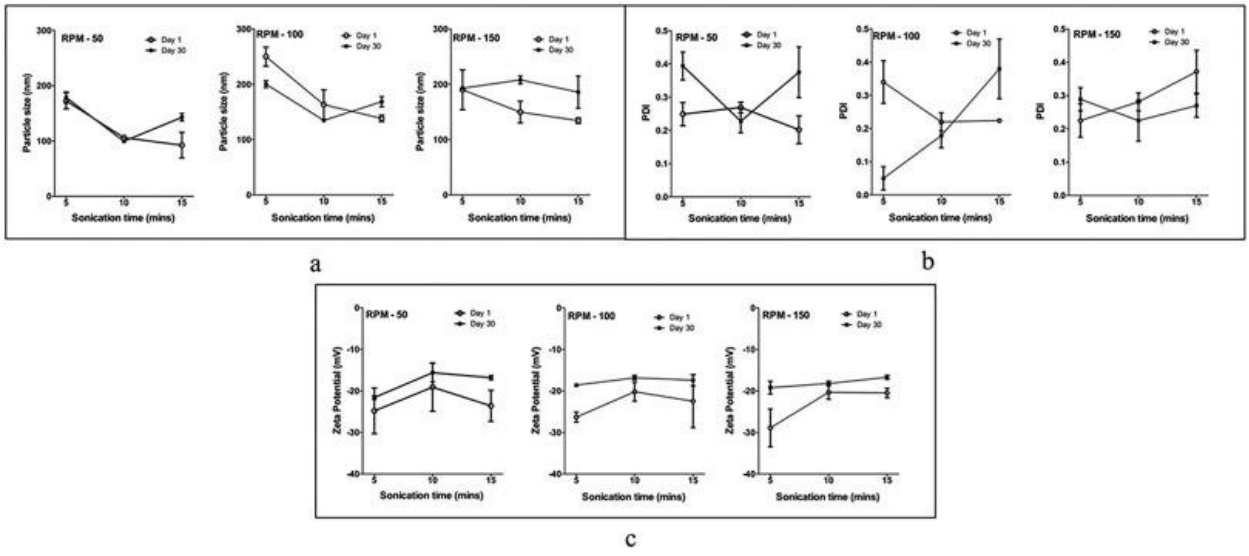

Figure 14. Effect of parameters on attributes of the formulation. 14a- Effect of parameters on the particle size of formulation. 14b- Effect of parameters on the PDI of the formulation. 14c- Effect of parameters on the zeta potential of the formulation.

From the between subject effects, it was observed that particle size was significantly affected by the screw speed and sonication time together which is evident from ***rpm*mins*** interaction ($p < 0.001$). The ***rpm*mins*** did not have a significant effect on the particle size ($p = 0.132$), but ***rpm*** ($p = 0.040$) and ***mins*** ($p = 0.011$) independently had a significant effect on PDI. While in case of zeta potential, only ***mins*** had a significant effect ($p < 0.002$), while ***rpm*** ($p = 0.941$) and ***rpm*mins*** interaction did not show any significant effect ($p = 0.734$).

The increase in particle size on storage observed for screw speed of 100 rpm and 150 rpm was due to decrease in residence time of the materials inside the barrel which limited the mixing of the aqueous and lipid phase during formation of pre-emulsion. In case of the probe sonication, with the increase in time a decrease in particle size of the formulation is observed. It is known that particles with lower size have higher surface free energy and need higher concentration of stabilizer [83]. In case of sonication time for 15 minutes on day 0 a lower particle size was observed

but on storage instability in the PEGylated NLC formulation is observed. As the formulation cools down during the longer sonication time, the NLCs start to solidify and the continuous energy input from the probe sonication breaks down these solidifying nanoparticles. These incompletely solidified NLCs on storage start exhibiting instability due to sedimentation and agglomeration.

Post-hoc analysis was performed to understand the main effects of the independent variables as well as the interaction. The formulation NLC-2 (screw speed – 50 rpm and sonication time - 10 mins) was selected for further evaluation as it showed the least particle size as well as it did not show any significant change in particle size, PDI and zeta potential on storage for 30 days ($p>0.05$).

3.4.4. Entrapment Efficiency and Assay

The percent entrapment efficiency for all the ITZ-PEG-NLC formulations investigated was between 95% and 98%. The percent entrapment efficiency of the ITZ-PEG-NLC obtained for formulation NLC-2 was 97.28 ± 0.50 %. The obtained assay (drug content) for all formulations was more than 95%. The assay of the NLC 2 formulation was found to be 96.40 ± 4.06%.

3.4.5. *In-vitro* drug release

The release profile of ITZ from the formulation (NLC-2) on day 0 and day 30 is presented in Fig. 15, The drug was released from the PEGylated nanoparticles with an initial burst release of 41.74 ± 1.49% in 1 h followed by a slower release for day 0 formulation. Similar results were observed with the initial burst release of 43.6 ± 0.5% in 1 h and then a controlled release for the stability formulation on day 30. The similarity factor (f_2) value for the day 0 and day 30 formulations was 70.17. The observed burst release could be due to the drug being loosely bound or near the surface. The drug at the center of the nanoparticle core was not released as nanoparticles

remained intact and maintained their integrity for the duration of the study. Thus, a plateau in drug release was observed after 24 h as the drug at the surface was released. This is consistent with the hypothesis of intracellular drug delivery; where after the initial burst, the nanoparticles will carry the drug into the cell on cellular uptake[84]. The nanoparticles degrade by activity of intracellular lipases and release the drug within the cell[85].

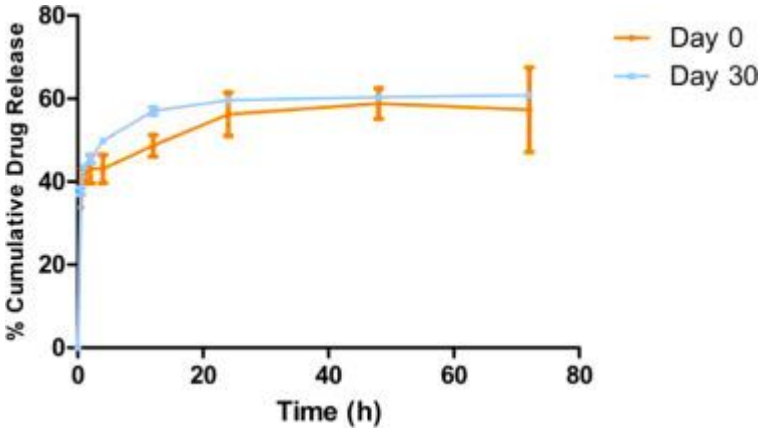

Figure 15. In vitro release of the ITZ-PEG-NLC in 10 mL of 20% 2-hydroxypropyl-beta cyclodextrin (mean ± SD, n=3)

3.4.6. Viscosity

From the Fig. 16, it was observed that the ITZ-PEG-NLC formulation showed decrease in viscosity with increasing spindle speed. During the nebulization processes a high shear is applied on the formulation to form aerosols. It has been shown that viscosity of the formulation plays an important role in determining the droplet size during nebulization[86]. Hence, it was necessary to determine the effect of shear on the viscosity of the formulation. The ITZ-PEG-NLC exhibited a non-Newtonian behavior and showed a decreasing trend on application of higher stress.

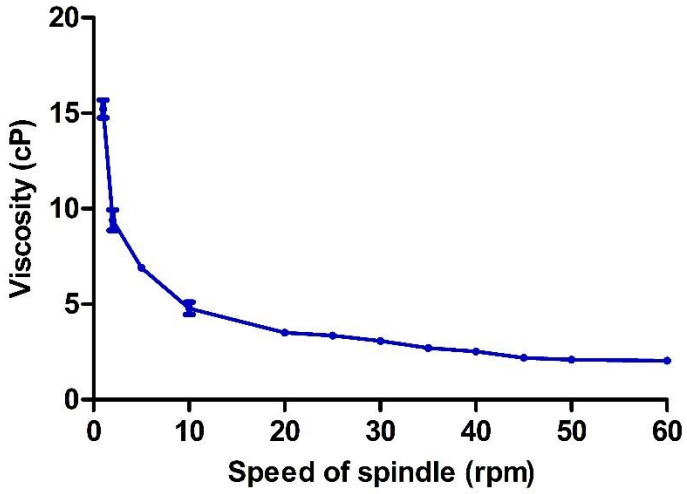

Figure 16. Viscosity against the speed of spindle (CPE 44) using the Brookfield cone and plate viscometer, (each error bar represents standard deviation, n=3).

3.4.7. Powder X-ray Diffraction Analysis

The Fig. 17, represents the PXRD stacked plots for the ITZ, ITZ-PEG-NLC and the placebo-PEG-NLC. The sharp PXRD peaks for ITZ indicated crystalline nature. The PXRD plots revealed the absence of characteristic ITZ peaks at 2θ values of 14.5θ and between 17θ -19θ in the ITZ-PEG-NLC. The sharp peak intensity at 20.5θ of the ITZ was substantially reduced in the ITZ-PEG-NLC. As the drug was completely solubilized in the lipid matrix, the crystallinity of the drug was lost, and a homogenous formulation was achieved with the amorphous nature of ITZ in the formulation. This observation is in accordance with reported studies[87,88].

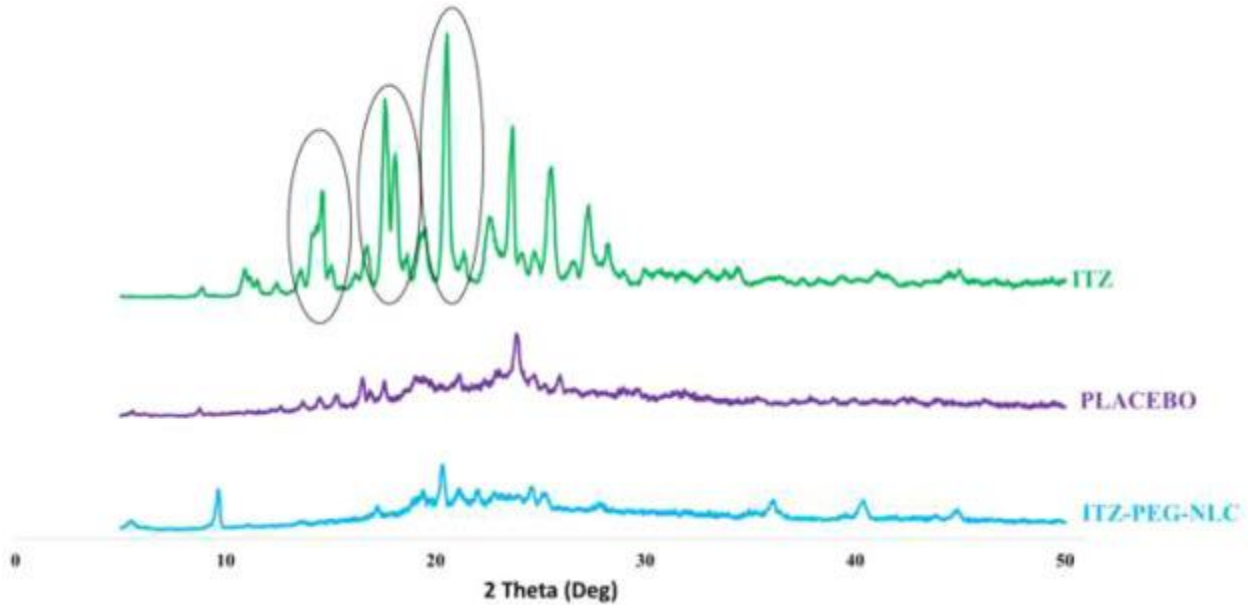

Figure 17. PXRD Diffractograms of pure ITZ, ITZ-PEG-NLC formulation (F-2) and placebo formulation.

3.4.8. Nebulization of the ITZ-PEG-NLC

Before nebulization of the PEGylated NLC formulation using the Philips Respironic Sami the Seal Nebulizer Compressor, the obtained particle size was 101.20 ± 1.69 nm with a PDI of 0.26 ± 0.02. The entrapment efficiency observed was 97.28 ± 0.50 %. After nebulization, the obtained particle size, PDI and entrapment efficiency was 103.56 ± 5.60, 0.25 ± 0.04 and 97.14 ± 0.89 %, respectively. This test was carried to observe the effect of jet nebulizer on the aerosolization of the PEGylated NLC formulation. It is known that during the jet nebulization of the PEGylated NLC formulation, due to the shear forces generated it can disturb the structural integrity of the nanoparticles, agglomerate or aggregate thus leading to instability[89]. Figure 18 shows the particles size and PDI of the ITZ-PEG-NLC before and after nebulization of PEGylated NLC formulation using Philips Respironics Sami the Seal Nebulizer Compressor. From, the

observed effect, we can conclude that the PEGylated NLC formulation was stable even after nebulization.

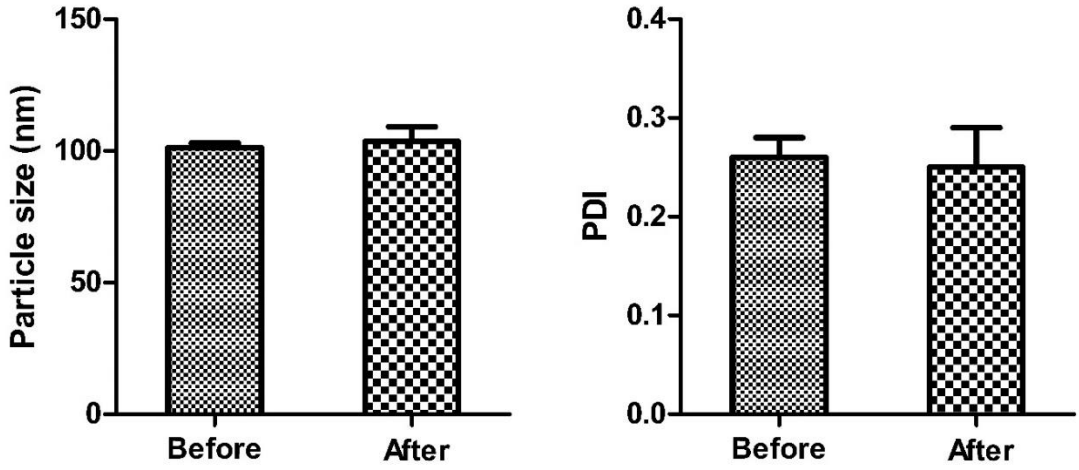

Figure 18. Particle size and PDI of the PEGylated NLC formulation before and after nebulization, $p>0.05$

3.4.9. Aerodynamic characterization

The aerodynamic characteristics of the ITZ-PEG-NLC formulation was determined using Anderson Cascade Impactor (ACI) and Philips Respironics Sami the Seal Nebulizer and Compressor. The amount of ITZ deposited over the seven stages of Anderson Cascade impactor is summarized in Figure 19. Determination of aerodynamic properties of the NLC formulation is essential to determining the extent of NLC delivery to the lungs after nebulization. The MMAD obtained is less than 5 µm which is within the specified inhalable range. The variability in the particle diameter within the aerosol is measured by GSD. The results showed the MMAD of 3.517 ± 0.28 µm, FPF of 52.23 ± 7.07%, and GSD of 2.44 ± 0.49 the PEGylated NLC-2 formulation. The MMAD of the formulation is an important parameter as it determines the amount of drug deposition in the lung. For inhalation drug delivery the particle size of the formulation should be

in the range of 1 µm to 5 µm for optimal deep lung delivery. Particles in the range of >5 µm after inhalation are deposited in the conducting airways and oropharyngeal region while <1 µm can get exhaled[90]. The variability in the particle diameter within the aerosol is measured by GSD; the results showed that the formulation was a hetero-disperse aerosol (GSD > 1.2). This was observed by distribution of the formulation at different stages in the ACI. A higher percent of FPF ensures efficient delivery of dose to the deeper lung tissues.

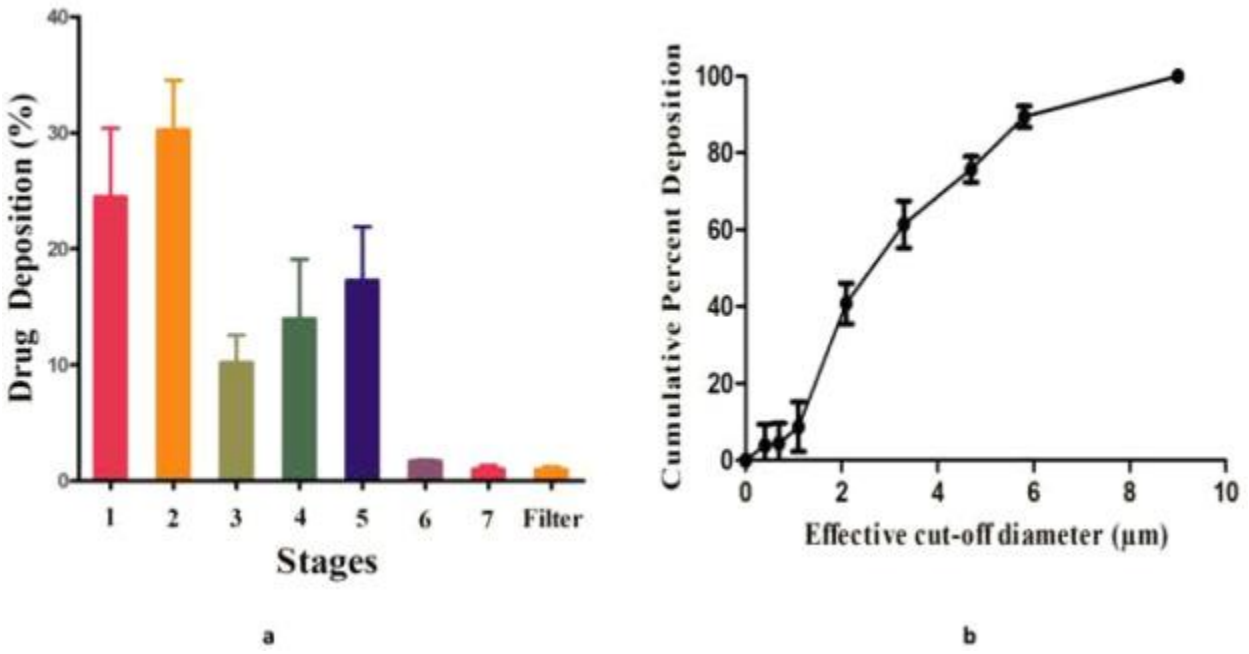

Figure 19. a-Amount of ITZ deposited on each stage of Anderson Cascade Impactor using the Philips Respironics Sami the Seal Nebulizer Compressor; b-Cumulative mass deposition versus the Anderson Cascade Impactor effective cut-off diameters, (each error bar represents standard deviation, n=3).

The recovered formulation was 85.57 ± 2.98 %. The obtained results from the developed ITZ-PEG-NLC formulation showed that the nanoparticles possess acceptable aerosolization properties and are suitable for deep lung tissues.

3.4.10. Safety of NLC formulation and placebo in epithelial A549 cells

It is important to determine the safety of the formulation when in contact with lung epithelial cells. The cytotoxicity of the ITZ-PEG-NLC and placebo PEG-NLC formulations was determined using A549 cells by incubation at various formulation concentrations for 24, 48, and 72 h (Fig. 20). The cells were treated with ITZ-PEG-NLC, and PEG-Placebo diluted 500-, 1000-, and 2000-times (0.5 µg/mL, 0.25 µg/mL, 0.125 µg/mL respectively) to match the *in vivo* dilution on dosing. The treated cells did not show any significant difference ($p > 0.05$) in cell viability when compared to the untreated cells (control). *In vitro* cell viability results showed no direct relationship between ITZ concentration and exposure time, demonstrating the safety of the formulation. From the obtained results we can say that this formulation can be used for longer duration of treatment as no toxic effects of the formulation were seen on the cells on continuous exposure for up to 48 h.

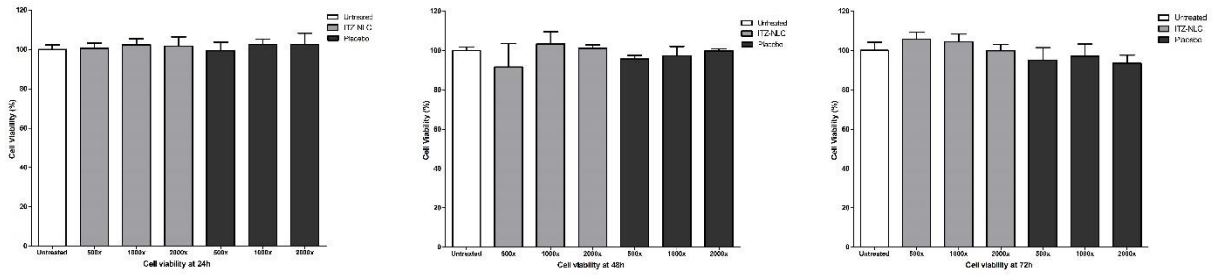

Figure 20. Cell viability measured by the crystal violet assay for the ITZ-PEG-NLC against the A549 cell line.

3.4.11. Spherical shape of NLC

Tandem Electron Microscopy was performed on the ITZ-PEG-NLC formulation F2 to understand the shape and morphology of the NLCs. From the Fig. 21 we can say that the

PEGylated NLC are spherical, and the particle size observed is similar to the particle size obtained from the dynamic light scattering.

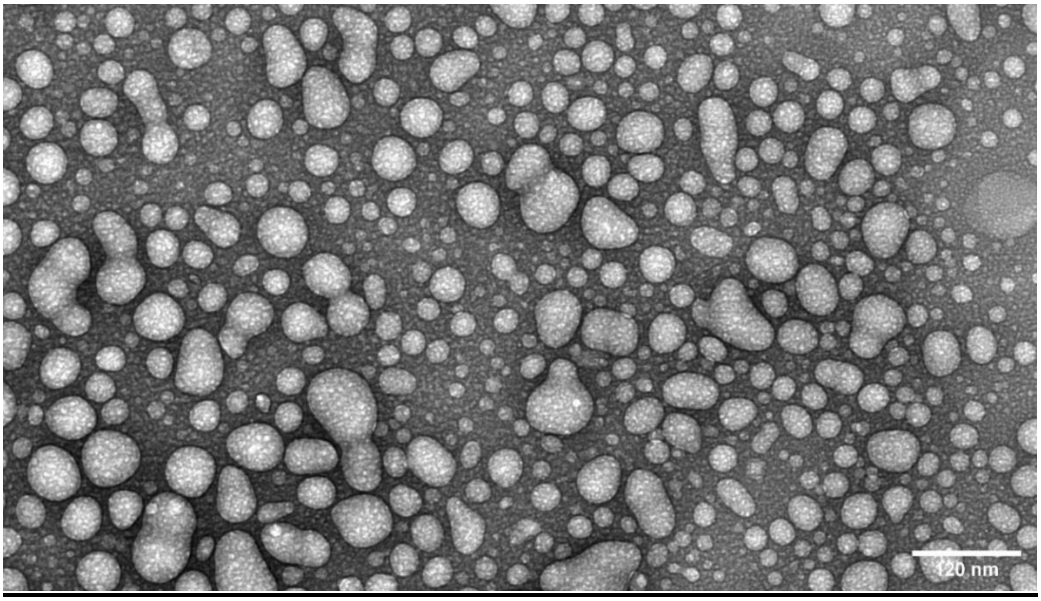

Figure 21. Tandem Electron Microscopy of the NLC formulation (F2)

3.5. CONCLUSION

PEGylated itraconazole NLC was prepared using HME along with probe sonication. Continuous production of NLCs can be achieved by this method by optimizing the parameters of HME such as screw speed, screw design, and barrel temperature. Utilizing this method minimizes the issues and variations associated with conventional batch methods of nano-formulations production. Our experiments demonstrated that the process parameters influence the formulation quality, with pre-emulsion largely determining the final quality of the formulation. A formulation method for preparing nanoscale particles having high entrapment efficiency and NLCs with good aerosolization properties was developed. The formulation was nebulized without aggregation and agglomeration. The drug formulation was found to be nontoxic to epithelial lung cells. TEM particles showed the spherical nature of the particles. We conclude that the formulation of

itraconazole PEGylated nanoparticles prepared by using HME technology may be considered as a potential pulmonary drug delivery system with manufacturing scalability.

CHAPTER IV

DEVELOPMENT OF SOLID SELF MICROEMULSIFYING DRUG DELIVERY SYSTEMS USING HOT-MELT EXTRUSION TECHNOLOGY

4.1. INTRODUCTION

Low bioavailability due to poor aqueous solubility and dissolution rate is exhibited generally by poorly water-soluble drugs[92]. For the development of oral dosage form products, the approaches to increase solubility or dissolution rate of these drugs for optimal bioavailability are needed[93]. Among several approaches reported in the literature, self-micro emulsifying drug delivery system (SMEDDS) offers the potential for enhancing absorption and subsequently the better bioavailability of poorly water-soluble drugs by presenting the drug in solubilized form in the gastrointestinal tract (GIT)[94,95]. SMEDDS is defined as an isotropic mixture of oils, surfactants/co-surfactants and drug, which rapidly forms nano emulsion with droplet size typically less than 200 nm upon oral administration into the GIT[96,97]. The formed micro emulsion enhances drug solubilization by incorporating the drug in lipid/surfactant colloidal aggregates formed upon contact with aqueous medium[98]. SMEDDS have exhibited an interesting role in oral delivery of highly lipophilic drugs due to ease of production, enhancement of drug solubility and oral bioavailability[99]. Other advantages of SMEDDS in enhancing oral bioavailability of lipophilic drugs consists of facilitating transcellular and paracellular absorption, reducing cytochrome-P450 metabolism in the gut enterocytes, promoting lymphatic transport via Peyer's patches protects drug from hepatic first pass metabolism[100,101].

However, the traditional liquid self-micro emulsifying drug delivery systems (SMEDDS) have limitations such as low drug loading capacity, drug leakage, low stability, excipient-capsule

incompatibility, possibility of irreversible drugs/excipients precipitation and high production cost[102,103]. To overcome these complications in the previous approach liquid SMEDDS are usually adsorbed on to inert carriers to produce solid SMEDDS (S-SMEDDS)[104]. This approach of S-SMEDDS has advantages like stability, facility of manufacturing process, accuracy and patient compliance. Thus incorporation of liquid SMEDDS into solid dosage forms combines the advantages of lipid based drug delivery systems with those of solid dosage forms.

Hot-melt extrusion (HME) technology is a continuous process of pumping raw materials at high temperatures and pressures to obtain a uniform product[105,106]. HME offers many advantages over conventional pharmaceutical manufacturing processes as it eliminates the use of solvents, it provides environmental advantages along with shorter and efficient processing time to produce the final product[107,108]. HME has been successfully used to enhance the solubility, bioavailability with higher drug loading in poorly water-soluble drugs[109].

Indomethacin (IND) (Fig.22) is a typical BCS class II drug with poor water-soluble property and has been frequently used to act as a model drug in numerous studies involving hot-melt extrusion (HME) technology[110]. It has a molecular weight of 357.8 g/mol and logP of 4.27 with melting temperature of 162°C[111].

Thus, the current study was aimed to develop S-SMEDDS for IND as a potential drug delivery system using the HME technique using solid surfactant and oils without need for any carrier matrix. Until now, there has not been any research article investigating preparation of lipid-based S-SMEDDS using HME.

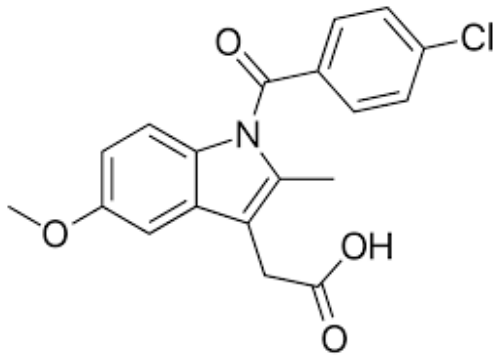

Figure 22. Indomethacin (IND) molecular structure

4.2. MATERIALS

Indomethacin (> 98% purity) was purchased from TCI Chemicals (Tokyo, Japan). Capryol® 90 (Propylene glycol monocaprylate), Lauroglycol™ FCC (Propylene glycol monolaurate-type-I) and Transcutol® HP (Diethylene glycol monoethyl ether) were obtained as gift samples from Gattefosse (Saint-Priest Cedex, France). Capmul® MCM (medium chain mono-and diglycerides) was purchased from Abitec (Janesville, Wisconsin, USA). Poloxamer 188 (Pluronic F68) and Castor oil were purchased from Acros Organics (Morris, NJ, USA). All other chemicals used in this study and solvents were of analytical or HPLC grade respectively.

4.3. METHODS

4.3.1. Solubility of indomethacin in lipids and surfactants

The lipids with high drug solubility for IND were selected as reported in literature[112]. To access the solubility of IND in the lipid-surfactant-cosurfactant mixture, 100 mg of IND was added to the mixture of lipid, surfactant and co-surfactant in fixed ratio. This mixture was kept for stirring on a magnetic plate overnight at 40°C. The lipid mixtures with clear consistency were allowed to

cool down and solidify. On solidification, 100 mg of the mixture was added to 20 mL of deionized water. The mixtures yielding clear emulsions were selected for further development.

4.3.2. Hot melt extrusion method

For the preparation of S-SMEDDS, hot-melt extruder (11 mm Process 11, Thermo Fisher Scientific, Karlsruhe, Germany) with a modified screw configuration (Fig. 23) was utilized. The modified screw configuration provided efficient mixing of the solid mixture with the liquid part of the formulation. The volumetric feeder and peristaltic pumps were calibrated depending on to suit the ratio of the solid content (IND and Poloxamer 188) and liquid content (lipid and co-surfactant) in the formulation. Table 12 lists the number of runs with the total content of the IND, lipid and surfactants. A schematic illustration of the IND S-SMEDDS formulation by the HME is shown in Fig. 24. All the materials were exposed to efficient mixing before the ejection of the formulation.

The drug was uniformly mixed with Poloxamer 188 using a V-shell blender (Maxiblend®, GlobePharma, New Brunswick, NJ, USA) and introduced into the barrel using a volumetric feeder. Selected lipid and the co-surfactant mixtures were at the temperature equivalent to the extrusion temperature were added into the barrel using a peristaltic pump in zones 2. The barrel temperature for zones 1 to 4 was 65°C, for zone 5 and 6 was 45°C and for zones 7-8 it was 30°C. The screw speed was kept constant at 50 rpm for all the runs to allow for higher residence time and uniform mixing of the IND, lipid and surfactants. The solid extrudate ejected from the HME was collected.

Table 12. Formulation prepared using HME with the contents

Run Number	**Lipid (mg)**		**Drug Content (mg)**	**Transcutol® HP (mg)**	**Poloxamer 188 (mg)**
1	Lauro glycol	200	0	200	700
2	FCC™	200	50	200	700
3		200	100	200	700

4	Capryol® 90	200	0	200	700
5		200	50	200	700
6		200	100	200	700
7	Capmul®	200	0	200	700
8	MCM	200	50	200	700
9		200	100	200	700
10	Castor oil	200	0	200	700
11		200	50	200	700
12		200	100	200	700

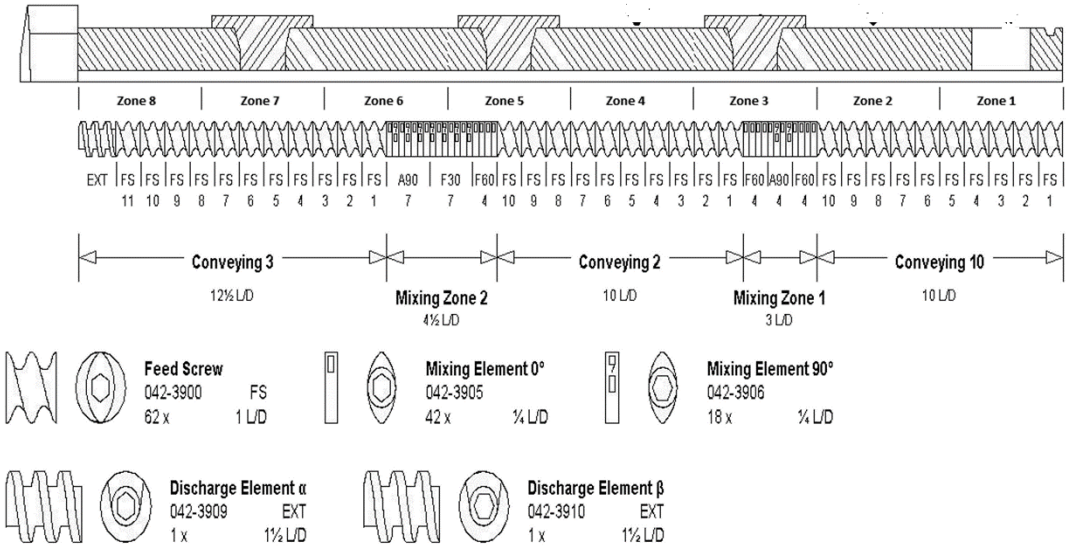

Figure 23. Screw configuration utilized for the HME process to prepare S-SMEDDS of IND.

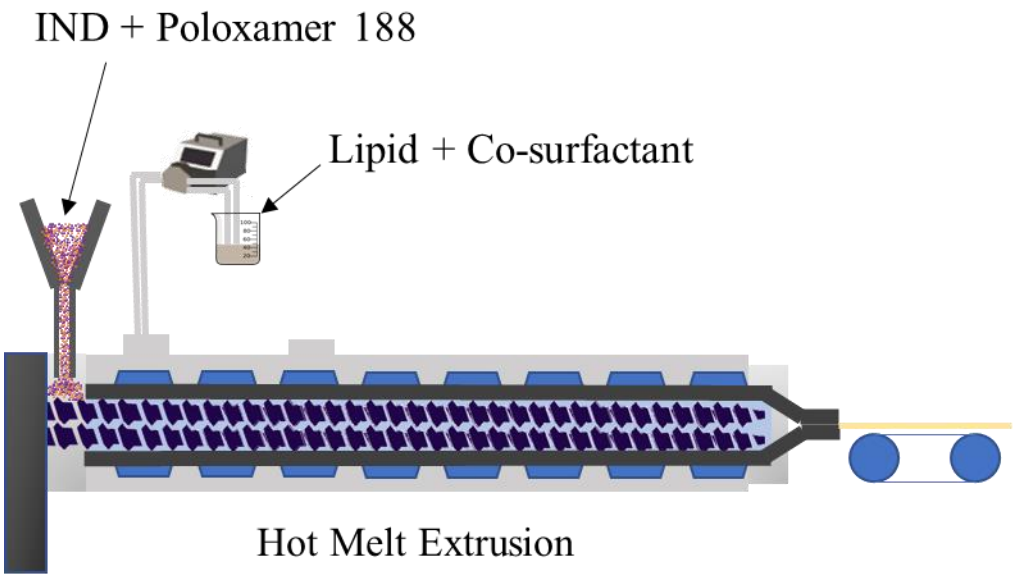

Figure 24. A schematic illustration of IND S-SMEDDS formulation by HME

4.3.3. Globule size, PDI, zeta potential and drug content

The globule size, PDI, and zeta potential of the formulations were determined by photon correlation spectroscopy using a Zetasizer Nano ZS Zen3600 (Malvern® Instruments, Malvern, UK) at a temperature of 25°C and with 173° backscatter detection in disposable folded capillary clear cells. The measurements were obtained using a helium-neon laser, and the particle size data were evaluated based on the volume distribution. Briefly, 100 µL of the sample was diluted to 1000 µL using deionized water, and the particle size and PDI were measured. For the drug content of the prepared S-SMEDDS, from each prepared formulations 100 mg was weighed and dissolved in 100 mL of acetonitrile water solution (1:1). This was diluted 50 times using acetonitrile and analyzed for the concentration using ultraviolet (UV) spectrophotometer (GENESYS 180, Thermo Fisher Scientific, Waltham, MA, USA) at 235 nm. The results were extrapolated from the standard curve to determine drug content.

4.3.4. Dissolution study

The relative *in vitro* dissolution behavior of IND from pure IND and S-SMEDDS in 0.1 N hydrochloric acid (900 mL; pH 1.2; 37 ± 0.5°C) was assessed using USP type II apparatus (paddle type; Hanson SR8-Plus, Chatsworth, CA, USA) at a paddle rotation speed of 50 rpm. IND equivalent to 100 mg of S-SMEDDS was added into the dissolution apparatus. At predetermined time points, an aliquot of 1 mL was withdrawn with equal volumes of fresh dissolution medium replacements to maintain the medium volume constant. All the samples were filtered, diluted and the concentration of indomethacin dissolved was assayed by UV spectroscopy (GENESYS 180, Thermo Fisher Scientific, Waltham, MA, USA) at 235nm.

4.3.5. Differential scanning calorimetry (DSC)

Thermal analysis of pure IND, placebo S-SMEDDS, and the S-SMEDDS formulation at 100 mg were carried out to determine the physical state of IND in the developed formulations using DSC (DSC 25, TA instruments, New Castle, DS, USA), calibrated with indium (calibration standard, purity >99.9%). Accurately weighed sample (~ 4 mg) was placed in a flat-bottomed standard aluminum pan and scanned at a scanning speed of 10°C/min from 25°C to 200°C under nitrogen gas flow of 50 mL/min.

4.3.6. Statistical analysis

All the data expressed as mean ± standard deviation (SD) was subjected to statistical analysis using JASP 0.13.1.0 software by one way analysis of variance (ANOVA). The differences were considered to be significant at $P < 0.05$.

4.4. RESULTS AND DISCUSSION

4.4.1. Hot-melt Extrusion

Data obtained from literature and solubility testing, Lauroglycol™ FCC, Capmul® MCM, Capryol® 90 and Castor oil were the lipids used in the study. Poloxamer 188 and Transcutol® HP were surfactant and co-surfactant respectively. A modified screw design, with a mixing element after zone 1 and 2, was efficient in mixing of lipid with the surfactant and IND before ejection of the product from the barrel. Preliminary runs were performed to decide the temperature range of barrel and the operating design. The barrel temperature for all of the zones was optimized based on the thermal analysis of the physical mixture. The zone 1 temperature was higher than the rest of the barrel to facilitate efficient mixing of IND within the components as higher temperature caused a decrease in melt viscosity. For all the HME runs, the feeding rate and torque were controlled to prevent formulation variations. The obtained extrudates from the barrel had wax like consistency but solidified on cooling at room temperature.

4.4.2. Globule size, PDI, zeta potential

Table 13. Globule size, PDI for the prepared S-SMEDDS

Formulation No.	**Lipid**	**Globule size (nm)**	**PDI**	**Zeta Potential (mV)**	**Drug Content (%)**
F1	Lauroglycol™ FCC	237.07 ± 0.75	0.28 ± 0.01	-27.50 ± 0.56	-
F2	Lauroglycol™ FCC	209.53 ± 0.50	0.22 ± 0.03	-22.53 ± 0.75	95.73 ± 0.23
F3	Lauroglycol™ FCC	281.53 ± 19.45	0.20 ± 0.04	-25.87 ± 0.35	99.89 ± 4.35

F4	Capryol® 90	119.23 ± 2.54	0.24 ± 0.02	-22.70 ± 1.97	-
F5	Capryol® 90	124.53 ± 5.20	0.14 ± 0.04	-24.40 ± 1.76	100.49 ± 4.35
F6	Capryol® 90	104.00 ± 2.97	0.40 ± 0.04	-26.50 ± 1.54	99.20 ± 2.20
F7	Capmul® MCM	358.13 ± 190.4	0.62 ± 0.19	-0.19 ± 0.22	-
F8	Capmul® MCM	166.13 ± 14.23	0.65 ± 0.04	-6.82 ± 5.54	102.84 ± 1.65
F9	Capmul® MCM	167.87 ± 13.90	0.42 ± 0.18	-8.90 ± 4.76	97.54 ± 2.63
F10	Castor oil	152.20 ± 2.95	0.29 ± 0.01	-23.67 ± 0.75	-
F11	Castor oil	141.27 ± 0.59	0.27 ± 0.02	-23.13 ± 0.42	100.83 ± 3.03
F12	Castor oil	151.27 ± 4.68	0.31 ± 0.02	-23.20 ± 3.64	101.26 ± 1.55

From the above table (Table 13) and Fig. 25 and 26, it can be seen that the formulations containing Capmul® MCM exhibited a highest variation in globule size and PDI when compared to the other oil at different drug loading. In case of Lauroglycol™ FCC, the formulation containing 100mg of Indomethacin showed highest globule size and the globule size for placebo and formulation containing 50 mg drug were both more than 200 nm. The formulations containing Capryol® 90 had the smallest globule size among all oils and exhibited a small PDI as well. All the lipid formulations except that of Capmul® MCM, exhibited a zeta potential more than – 20mV (Figure 27). The drug content for all the formulation was more than 95%.

Table 14. ANOVA analysis for globule size, PDI and zeta potential with p values for the analysis

Cases	Globule size	PDI	Zeta potential
Lipid	< .001	< .001	< 0.001
Indo	0.036	0.487	0.052
Lipid*IND	0.016	0.001	0.01

This current study examined if a relationship between type of lipid (*lipid*) and the drug loading (*IND*) in the formulation on the globule size and PDI of the S-SMEDDS formulations. Given the categorical nature of type of lipid, this current study employed a two-way ANOVA rather than a regression analysis. An alpha level of 0.05 was utilized and the homogeneity of variance assumption was met, and groups were normally distributed. The type of lipid used (*lipid*) had a significant effect on the globule size ($p < 0.001$) as well as PDI ($p < 0.001$) and Zeta potential ($p < 0.001$) of the S-SMEDDS (Table 3). The drug loading (*IND*) had a significant impact on the globule size ($p = 0.036$) of the S-SMEDDS while no significant effect of (*IND*) was observed on the PDI (($p = 0.487$) and zeta potential ($p = 0.052$). The interaction of the type of lipid and the drug loading (*lipid*IND*) was found to be significant for both globule size ($p < 0.016$), PDI ($p = 0.001$) and zeta potential ($p = 0.01$)

Hence to understand effect of each lipid and the different levels of drug loadings on the globule size, PDI and zeta potential the Simple Main effects for the ANOVA analysis were investigated.

Table 15. Simple effects of different lipids on drug loading with p values for the analysis

Level of IND	Globule size	PDI	Zeta Potential
0	< 0.001	< 0.001	< 0.001
50	0.289	<0.001	< 0.001
100	0.005	0.009	< 0.001

From the Simple Main effects for the type of lipid in the formulation on the different levels of drug loading (Table 15) it was seen that there was significant difference between globule size of the placebo formulations ($p < 0.001$) and formulations with 100mg of drug loading ($p < 0.005$). The difference in the globule size seen in the case of the placebos can be attributed to the behavior of each individual lipids in the S-SMEDDS system. The non-significant difference ($p = 0.289$) in globule size observed for the 50 mg drug loading can be attributed to the complete solubilization of drug and efficient emulsification of the S-SMEDDS system. In case of the PDI, the different types of lipids had a significant effect on all the three drug loadings of the S-SMEDDS formulations, placebo ($p < 0.001$), formulations with 50mg IND ($p < 0.001$) and formulations with 100 mg of drug loading (p 0.009). This can be explained from the significant interaction (*Lipid*IND*) seen between the type of lipid and drug loading and can be attributed to the behavior of the individual lipid in the surfactant system and solubility of the drug in the lipid. In case of the zeta potential for the formulations, a significant difference was seen for all the drug loadings, placebo ($p < 0.001$), 50 mg ($p < 0.001$) and 100mg ($p < 0.001$).

Table 16. Simple effects of drug loading on different lipids with p values for the analysis

Type of Lipids	Globule size	PDI	Zeta Potential
CMCM	< 0.001	0.002	< 0.001
CO	0.965	0.785	0.962
CP90	0.896	0.002	0.208
LFCC	0.296	0.446	0.07

From the simple main effects of the drug loading on each type of lipid (Table 16) it was seen that there was no significant effect on the globule size of formulation containing castor oil ($p = 0.965$) and Lauroglycol™ FCC ($p = 0.296$). PDI of the formulations with castor oil ($p = 0.785$) and Lauroglycol™ FCC ($p = 0.296$) was not significantly affected by different drug loadings. The

formulations containing Capmul® MCM exhibited significant increase in globule size ($p < 0.001$) with increasing drug loading as well as a corresponding increase in PDI ($p = 0.002$). The formulations with Capryol®90 did not exhibit significant difference in globule size ($p = 0.896$) but a had significant difference for PDI ($p = 0.002$) with different drug loadings. In case of the zeta potential of the formulations, only Capmul® MCM had a significant difference for the formulations with different drug loadings ($p < 0.001$) while all other lipids exhibited a non-significant difference.

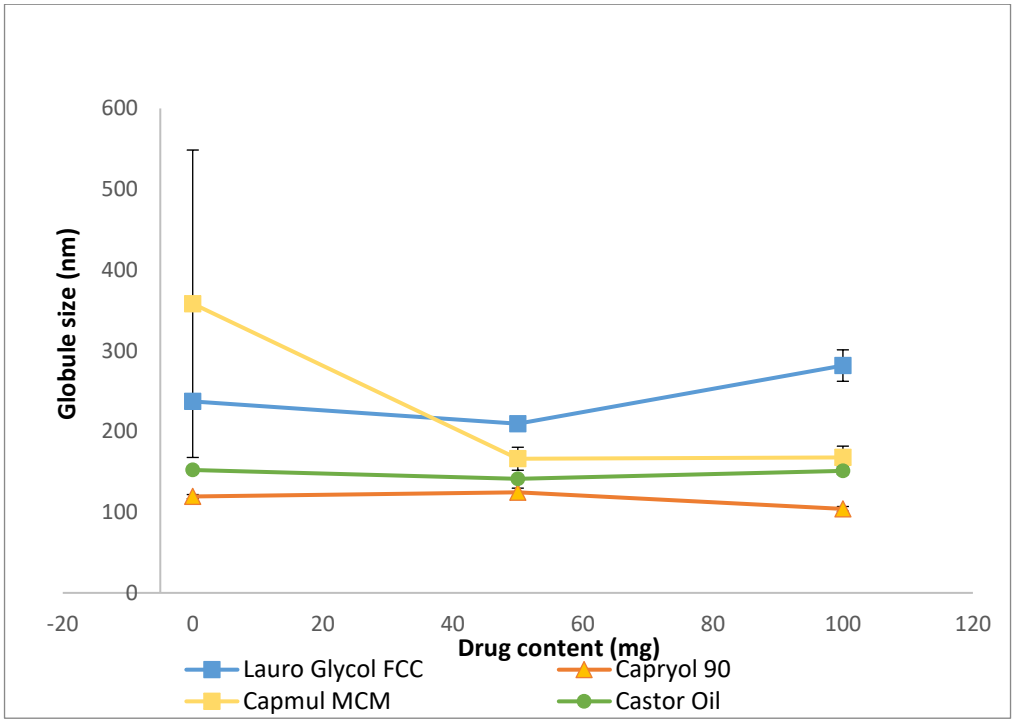

Figure 25. Effect of lipids on the globule size of the IND S-SMEDDS

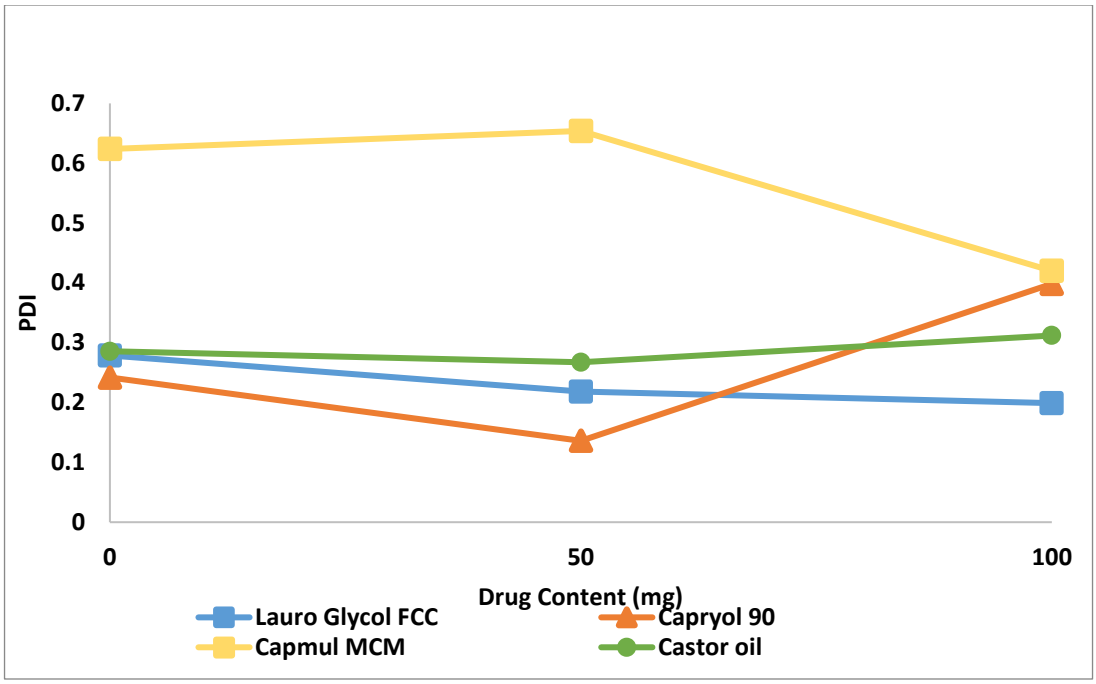

Figure 26. Effect of lipids on the PDI of the IND S-SMEDDS

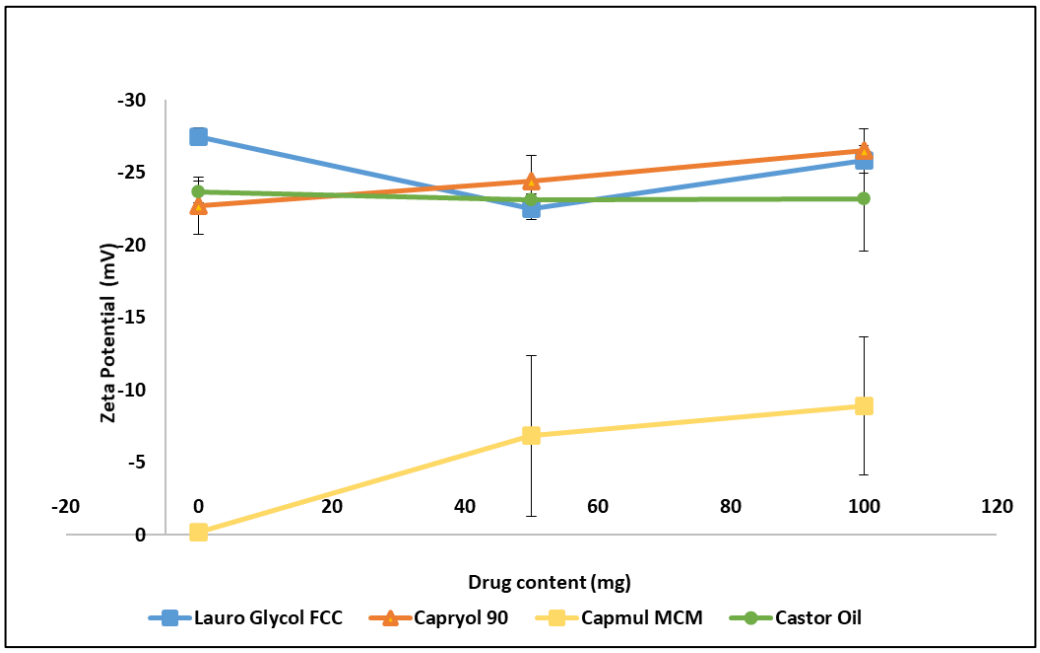

Figure 27. Effect of lipids on the Zeta potential of the IND S-SMEDDS

4.4.3. Dissolution study

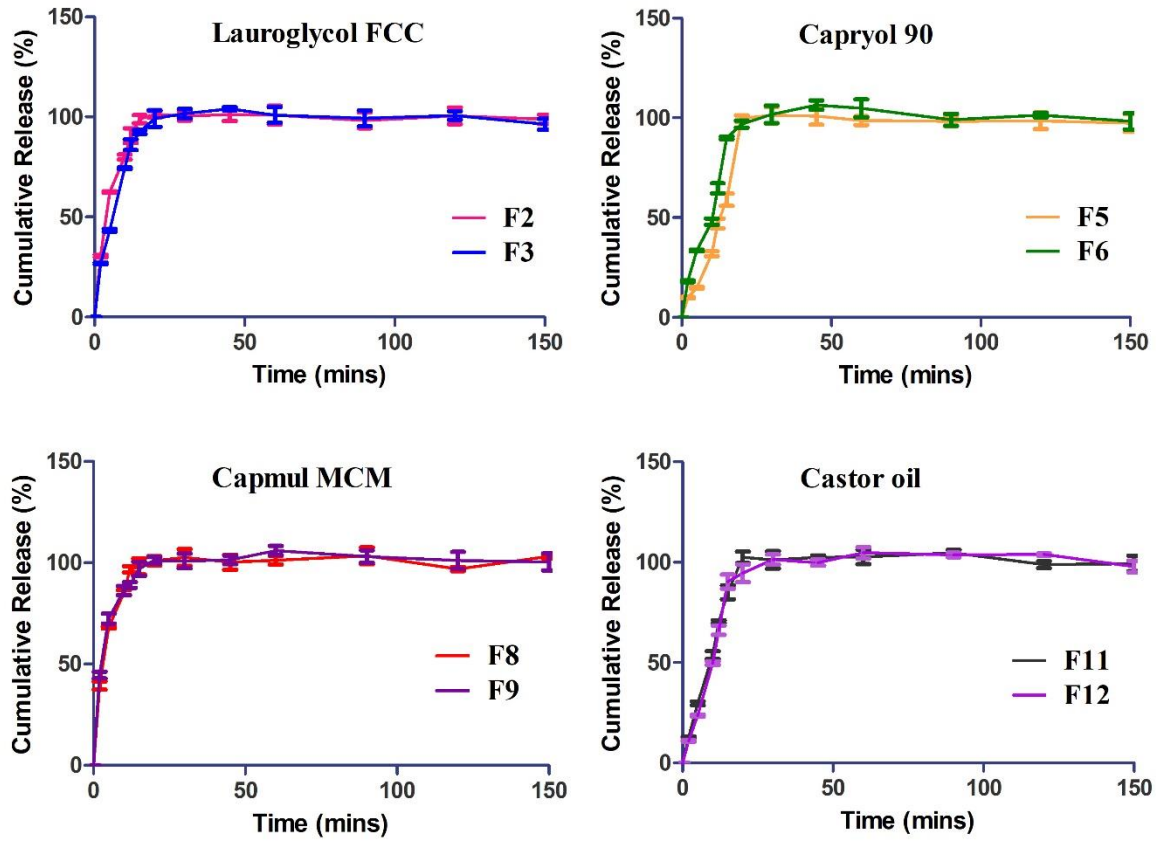

Figure 28. Dissolution study of IND S-SMEDDS

The self-emulsifying drug delivery systems on oral administration can undergo rapid emulsification to form o/w type emulsion in the gastro-intestinal fluid aided by the peristaltic motions of the GIT. The emulsion droplets due to their hydrophobic core, dissolve and trap the drug within them, and these droplets are stabilized by the surfactant-cosurfactants present in the formulation. Thus, there is solubility enhancement of the drug and precipitation in the GIT is prevented. The entrapment of the drug in the lipid matrix can also increase bioavailability of the drug.

The drug release study was performed in USP type II apparatus for a total duration of 150 mins. All the formulations exhibited a rapid emulsification of the matrix and thereby fast drug

release. Formulations containing Lauroglycol™ FCC and Capmul® MCM exhibited a comparatively faster release and reached about 100% cumulative concentration 15 mins (Figure 28). While in case of Capryol® 90 the drug release at 15 mins was 58.88 ± 3.13% and 89.92 ± 0.65 % for formulation F5 and F6 respectively. The formulations F5 and F6 reached 100% drug release by 20 mins. All the formulations exhibited stable emulsification and did not show precipitation till end of the study. The drug loading did not have any significant impact on the rate of release of drug. The quick onset of emulsification, enhanced solubilization of the drug.

4.4.4. Differential scanning calorimetry

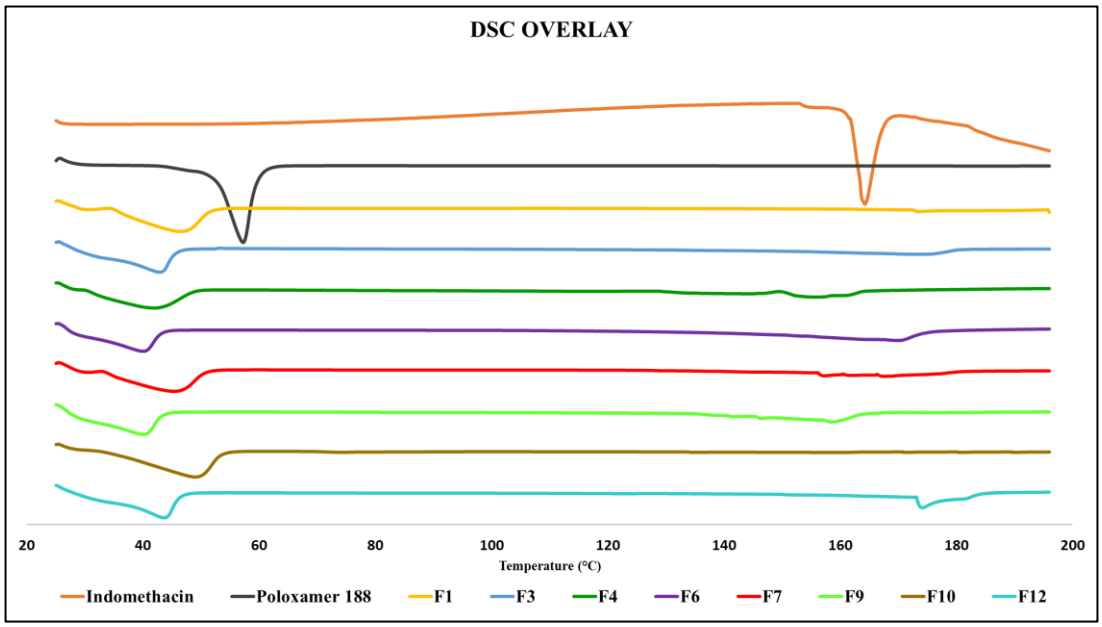

Figure 29. DSC Overlay of the prepared S-SMEDDS and pure IND

The prepared S-SMEDDS were characterized for the physical state of the IND in the S-SMEDDS by performing DSC analysis. The DSC thermogram of IND and Poloxamer 188 was recorded as shown in Fig. 29. Pure IND showed an endothermic peak at 160°C corresponding to its melting point. The poloxamer 188 showed a melting peak at 60°C.

Formulations, F1, F4, F7, F10 are the placebo formulations and F3, F6, F9 and F12 are the formulations containing 100 mg of IND. In all the IND containing formulations there is absence of conspicuous drug peak over the melting range unraveling the transformation of the physical state of the IND (crystalline to amorphous).

4.5. CONCLUSION

The current study is a step towards understanding the application of HME in preparation of S-SMEDDS. Increased residence time of the formulation due to low screw speed and high shear action imparted by the screw configuration was desirable for the preparation of S-SMEDDS. The formulation of S-SMEDDS composed of Capryol® 90 and castor oil gave desirable results. These developed S-SMEDDS could be a promising system for the oral bioavailability enhancement of a poorly soluble drug. Absence of crystalline solid state was concluded in the prepared S-SMEDDS.

This study is the first report on formulation preparation of S-SMEDDS with lipids using HME, which is a versatile, industrially feasible process that is gaining attention in the pharmaceutical manufacturing.

REFERENCES

1. Kerns EH. High throughput physicochemical profiling for drug discovery. *J Pharm Sci*. Published online 2001. doi:10.1002/jps.1134

2. Patil H, Tiwari R V., Repka MA. Hot-Melt Extrusion: from Theory to Application in Pharmaceutical Formulation. *AAPS PharmSciTech*. Published online 2016. doi:10.1208/s12249-015-0360-7

3. Alam MA, Ali R, Al-Jenoobi FI, Al-Mohizea AM. Solid dispersions: A strategy for poorly aqueous soluble drugs and technology updates. *Expert Opin Drug Deliv*. 2012;9(11):1419-1440. doi:10.1517/17425247.2012.732064

4. Leuner C, Dressman J. Improving drug solubility for oral delivery using solid dispersions. *Eur J Pharm Biopharm*. 2000;50(1):47-60. doi:10.1016/S0939-6411(00)00076-X

5. Serajuddln ATM. Solid dispersion of poorly water-soluble drugs: Early promises, subsequent problems, and recent breakthroughs. *J Pharm Sci*. 1999;88(10):1058-1066. doi:10.1021/js980403l

6. Crowley MM, Zhang F, Repka MA, et al. Pharmaceutical applications of hot-melt extrusion: Part I. *Drug Dev Ind Pharm*. Published online 2007. doi:10.1080/03639040701498759

7. Ashour EA, Majumdar S, Alsheteli A, et al. Hot melt extrusion as an approach to improve solubility, permeability and oral absorption of a psychoactive natural product, piperine. *J Pharm Pharmacol*. Published online 2016. doi:10.1111/jphp.12579

8. Kleinebudde P, Lindner H. Experiments with an instrumented twin-screw extruder using a single-step granulation/extrusion process. *Int J Pharm*. 1993;94(1-3):49-58. doi:10.1016/0378-5173(93)90008-4

9. Bhagurkar AM, Repka MA, Murthy SN. A Novel Approach for the Development of a Nanostructured Lipid Carrier Formulation by Hot-Melt Extrusion Technology. *J Pharm Sci*. Published online 2017. doi:10.1016/j.xphs.2016.12.015

10. Zhang J, Xu P, Vo AQ, et al. Development and evaluation of pharmaceutical 3D printability for hot melt extruded cellulose-based filaments. *J Drug Deliv Sci Technol*. 2019;52:292-302. doi:10.1016/j.jddst.2019.04.043

11. el-Egakey MA, Soliva M, Speiser P. Hot extruded dosage forms. I. Technology and dissolution kinetics of polymeric matrices. *Pharm Acta Helv*. Published online 1971.

12. Repka MA, Bandari S, Kallakunta VR, et al. Melt extrusion with poorly soluble drugs – An integrated review. *Int J Pharm*. Published online 2018. doi:10.1016/j.ijpharm.2017.10.056

13. Kalepu S, Nekkanti V. Insoluble drug delivery strategies: Review of recent advances and business prospects. *Acta Pharm Sin B*. Published online 2015. doi:10.1016/j.apsb.2015.07.003

14. Charalabidis A, Sfouni M, Bergström C, Macheras P. The Biopharmaceutics Classification System (BCS) and the Biopharmaceutics Drug Disposition Classification System (BDDCS): Beyond guidelines. *Int J Pharm*. 2019;566:264-281. doi:10.1016/j.ijpharm.2019.05.041

15. Zhang P, Shadambikar G, Almutairi M, Bandari S, Repka MA. Approaches for developing acyclovir gastro-retentive formulations using hot melt extrusion technology. *J Drug Deliv Sci Technol*. Published online August 15, 2020:102002. doi:10.1016/j.jddst.2020.102002

16. Patil H, Tiwari R V., Upadhye SB, Vladyka RS, Repka MA. Formulation and development of pH-independent/dependent sustained release matrix tablets of ondansetron HCl by a continuous twin-screw melt granulation process. *Int J Pharm*. 2015;496(1):33-41. doi:10.1016/j.ijpharm.2015.04.009

17. Vasconcelos T, Sarmento B, Costa P. Solid dispersions as strategy to improve oral bioavailability of poor water soluble drugs. *Drug Discov Today*. Published online 2007. doi:10.1016/j.drudis.2007.09.005

18. Muehlenfeld C, Thommes M. Miniaturization in pharmaceutical extrusion technology: Feeding as a challenge of downscaling. *AAPS PharmSciTech*. 2012;13(1):94-100. doi:10.1208/s12249-011-9726-7

19. Zecevic DE, Wagner KG. Rational development of solid dispersions via hot-melt extrusion using screening, material characterization, and numeric simulation tools. *J Pharm Sci*. Published online 2013. doi:10.1002/jps.23592

20. Tiwari R V., Patil H, Repka MA. Contribution of hot-melt extrusion technology to advance drug delivery in the 21st century. *Expert Opin Drug Deliv*. Published online 2016. doi:10.1517/17425247.2016.1126246

21. Agrawal AM, Dudhedia MS, Zimny E. Hot Melt Extrusion: Development of an Amorphous Solid Dispersion for an Insoluble Drug from Mini-scale to Clinical Scale. *AAPS PharmSciTech*. Published online 2016. doi:10.1208/s12249-015-0425-7

22. Cossé A, König C, Lamprecht A, Wagner KG. Hot Melt Extrusion for Sustained Protein Release: Matrix Erosion and In Vitro Release of PLGA-Based Implants. *AAPS PharmSciTech*. Published online 2017. doi:10.1208/s12249-016-0548-5

23. Sakai T, Thommes M. Investigation into mixing capability and solid dispersion preparation using the DSM Xplore Pharma Micro Extruder. *J Pharm Pharmacol*. Published online 2014. doi:10.1111/jphp.12085

24. Rask MB, Knopp MM, Olesen NE, Holm R, Rades T. Comparison of two DSC-based methods to predict drug-polymer solubility. *Int J Pharm*. Published online 2018. doi:10.1016/j.ijpharm.2018.02.002

25. Lin D, Huang Y. A thermal analysis method to predict the complete phase diagram of drug-polymer solid dispersions. *Int J Pharm*. 2010;399(1-2):109-115. doi:10.1016/j.ijpharm.2010.08.013

26. Kyerematen SO, Pudlas M, Woehrle GH. A fast and reliable empirical approach for estimating solubility of crystalline drugs in polymers for hot melt extrusion formulations. *J Pharm Sci*. 2014;103(9):2847-2858. doi:10.1002/jps.23941

27. Mohan R, Lorenz H, Myerson AS. Solubility measurement using differential scanning calorimetry. *Ind Eng Chem Res*. 2002;41(19):4854-4862. doi:10.1021/ie0200353

28. Lauer ME, Maurer R, De Paepe AT, et al. A miniaturized extruder to prototype amorphous solid dispersions: Selection of plasticizers for hot melt extrusion. *Pharmaceutics*. Published online 2018. doi:10.3390/pharmaceutics10020058

29. Auch C, Harms M, Mäder K. Melt-based screening method with improved predictability regarding polymer selection for amorphous solid dispersions. *Eur J Pharm Sci*. Published online 2018. doi:10.1016/j.ejps.2018.08.035

30. Chiang PC, Ran Y, Chou KJ, et al. Evaluation of drug load and polymer by using a 96-well plate vacuum dry system for amorphous solid dispersion drug delivery. *AAPS PharmSciTech*.

Published online 2012. doi:10.1208/s12249-012-9795-2

31. Treffer D, Wahl PR, Hörmann TR, et al. In-line implementation of an image-based particle size measurement tool to monitor hot-melt extruded pellets. *Int J Pharm*. Published online 2014. doi:10.1016/j.ijpharm.2014.03.022

32. MacFhionnghaile P, Hu Y, Gniado K, Curran S, McArdle P, Erxleben A. Effects of ball-milling and cryomilling on sulfamerazine polymorphs: A quantitative study. *J Pharm Sci*. 2014;103(6):1766-1778. doi:10.1002/jps.23978

33. Eder S, Beretta M, Witschnigg A, et al. Establishment of a Molding Procedure to Facilitate Formulation Development for Co-extrudates. *AAPS PharmSciTech*. Published online 2017. doi:10.1208/s12249-017-0788-z

34. Isabell Immohr. 3rd European Conference on Pharmaceutics. In: *Lean and Efficient Development of a Pseudoephedrine Formulation Resistant to Conversion into Meth.* ; 2019.

35. Evans RC, Bochmann ES, Kyerematen SO, Gryczke A, Wagner KG. Holistic QbD approach for hot-melt extrusion process design space evaluation: Linking materials science, experimentation and process modeling. *Eur J Pharm Biopharm*. 2019;141:149-160. doi:10.1016/j.ejpb.2019.05.021

36. Narasimhan B. Mathematical models describing polymer dissolution: Consequences for drug delivery. *Adv Drug Deliv Rev*. 2001;48(2-3):195-210. doi:10.1016/S0169-409X(01)00117-X

37. Miller-Chou BA, Koenig JL. A review of polymer dissolution. doi:10.1016/S0079-6700(03)00045-5

38. Yoshioka M, Hancock BC, Zografi G. Inhibition of indomethacin crystallization in poly(vinylpyrrolidone) coprecipitates. *J Pharm Sci*. Published online 1995. doi:10.1002/jps.2600840814

39. Semjonov K, Kogermann K, Laidmäe I, et al. The formation and physical stability of two-phase solid dispersion systems of indomethacin in supercooled molten mixtures with different matrix formers. *Eur J Pharm Sci*. 2017;97:237-246. doi:10.1016/j.ejps.2016.11.019

40. Jelić D, Liavitskaya T, Vyazovkin S. Thermal stability of indomethacin increases with the amount of polyvinylpyrrolidone in solid dispersion. *Thermochim Acta*. 2019;676:172-176. doi:10.1016/j.tca.2019.04.011

41. Nokhodchi A, Javadzadeh Y, Siahi-Shadbad MR, Barzegar-Jalali M. The effect of type and concentration of vehicles on the dissolution rate of a poorly soluble drug (indomethacin) from liquisolid compacts. *J Pharm Pharm Sci*. Published online 2005.

42. De Jaeghere W, De Beer T, Van Bocxlaer J, Remon JP, Vervaet C. Hot-melt extrusion of polyvinyl alcohol for oral immediate release applications. *Int J Pharm*. Published online 2015. doi:10.1016/j.ijpharm.2015.07.009

43. Bioavailability enhancement using hot melt extrusion – with functional solutions from BASF. Accessed October 17, 2020. https://pharmaceutical.basf.com/global/en/drug-formulation/processes/hot-melt-extrusion.html

44. Patra CN, Priya R, Swain S, Kumar Jena G, Panigrahi KC, Ghose D. Pharmaceutical significance of Eudragit: A review. *Futur J Pharm Sci*. Published online 2017. doi:10.1016/j.fjps.2017.02.001

45. Co-Rotating Twin-Screw Extruders: Fundamentals - Hanser Publications. Accessed October 17, 2020. https://www.hanserpublications.com/Products/534-co-rotating-twin-screw-extruders-fundamentals.aspx

46. Otsuka M, Matsumoto T, Kaneniwa N. Effect of Environmental Temperature on Polymorphic Solid-State Transformation of Indomethacin during Grinding. *Chem Pharm Bull*. 1986;34(4):1784-1793. doi:10.1248/cpb.34.1784

47. Trasi NS, Byrn SR. Mechanically induced amorphization of drugs: A study of the thermal behavior of cryomilled compounds. *AAPS PharmSciTech*. 2012;13(3):772-784. doi:10.1208/s12249-012-9801-8

48. Zografi G, Crowley KJ. Cryogenic grinding of indomethacin polymorphs and solvates: Assessment of amorphous phase formation and amorphous phase physical stability. *J Pharm Sci*. 2002;91(2):492-507. doi:10.1002/jps.10028

49. Dissolution Testing of Immediate Release Solid Oral Dosage Forms | FDA. Accessed October

17, 2020. https://www.fda.gov/regulatory-information/search-fda-guidance-documents/dissolution-testing-immediate-release-solid-oral-dosage-forms

50. Franco P, De Marco I. Eudragit: A Novel Carrier for Controlled Drug Delivery in Supercritical Antisolvent Coprecipitation. *Polymers (Basel)*. 2020;12(1):234. doi:10.3390/polym12010234

51. Wlodarski K, Zhang F, Liu T, Sawicki W, Kipping T. Synergistic Effect of Polyvinyl Alcohol and Copovidone in Itraconazole Amorphous Solid Dispersions. *Pharm Res*. 2018;35(1). doi:10.1007/s11095-017-2313-1

52. Tres F, Treacher K, Booth J, et al. Indomethacin-Kollidon VA64 Extrudates: A Mechanistic Study of pH-Dependent Controlled Release. *Mol Pharm*. 2016;13(3):1166-1175. doi:10.1021/acs.molpharmaceut.5b00979

53. Terife G, Wang P, Faridi N, Gogos CG. Hot melt mixing and foaming of soluplus® and indomethacin. *Polym Eng Sci*. 2012;52(8):1629-1639. doi:10.1002/pen.23106

54. Praphawatvet T, Peters JI, Williams RO. Inhaled nanoparticles–An updated review. *Int J Pharm*. 2020;587:119671. doi:10.1016/j.ijpharm.2020.119671

55. Patlolla RR, Chougule M, Patel AR, Jackson T, Tata PNV, Singh M. Formulation, characterization and pulmonary deposition of nebulized celecoxib encapsulated nanostructured lipid carriers. *J Control Release*. Published online 2010. doi:10.1016/j.jconrel.2010.02.006

56. Pilcer G, Amighi K. Formulation strategy and use of excipients in pulmonary drug delivery. *Int J Pharm*. Published online 2010. doi:10.1016/j.ijpharm.2010.03.017

57. Patel G, Chougule M, Singh M, Misra A. Nanoliposomal Dry Powder Formulations. *Methods Enzymol*. 2009;464(C):167-191. doi:10.1016/S0076-6879(09)64009-X

58. Puglia C, Sarpietro MG, Bonina F, Castelli F, Zammataro M, Chiechio S. Development, characterization, and in vitro and in vivo evaluation of benzocaine- and lidocaine-loaded nanostructrured lipid carriers. *J Pharm Sci*. Published online 2011. doi:10.1002/jps.22416

59. Müller RH, Radtke M, Wissing SA. Nanostructured lipid matrices for improved

microencapsulation of drugs. *Int J Pharm*. Published online 2002. doi:10.1016/S0378-5173(02)00180-1

60. Kousha M, Tadi R, Soubani AO. Pulmonary aspergillosis: A clinical review. *Eur Respir Rev*. Published online 2011. doi:10.1183/09059180.00001011

61. Hope WW. Invasion of the alveolar-capillary barrier by Aspergillus spp.: Therapeutic and diagnostic implications for immunocompromised patients with invasive pulmonary aspergillosis. *Med Mycol*. Published online 2009. doi:10.1080/13693780802510232

62. Alvarez CA, Wiederhold NP, McConville JT, et al. Aerosolized nanostructured itraconazole as prophylaxis against invasive pulmonary aspergillosis. *J Infect*. Published online 2007. doi:10.1016/j.jinf.2007.01.014

63. Maertens J, Boogaerts M. The place for itraconazole in treatment. *J Antimicrob Chemother*. Published online 2005. doi:10.1093/jac/dki222

64. Pardeike J, Weber S, Haber T, et al. Development of an Itraconazole-loaded nanostructured lipid carrier (NLC) formulation for pulmonary application. *Int J Pharm*. Published online 2011. doi:10.1016/j.ijpharm.2011.07.040

65. Akkar A, Müller RH. Intravenous itraconazole emulsions produced by SolEmuls technology. *Eur J Pharm Biopharm*. Published online 2003. doi:10.1016/S0939-6411(03)00063-8

66. Suk JS, Xu Q, Kim N, Hanes J, Ensign LM. PEGylation as a strategy for improving nanoparticle-based drug and gene delivery. *Adv Drug Deliv Rev*. Published online 2016. doi:10.1016/j.addr.2015.09.012

67. Suk JS, Lai SK, Wang YY, et al. The penetration of fresh undiluted sputum expectorated by cystic fibrosis patients by non-adhesive polymer nanoparticles. *Biomaterials*. Published online 2009. doi:10.1016/j.biomaterials.2008.12.076

68. Forier K, Messiaen AS, Raemdonck K, et al. Transport of nanoparticles in cystic fibrosis sputum and bacterial biofilms by single-particle tracking microscopy. *Nanomedicine*. Published online 2013. doi:10.2217/nnm.12.129

69. Lai SK, Wang YY, Hanes J. Mucus-penetrating nanoparticles for drug and gene delivery to mucosal tissues. *Adv Drug Deliv Rev*. Published online 2009. doi:10.1016/j.addr.2008.11.002

70. Palacio J, Agudelo NA, Lopez BL. PEGylation of PLA nanoparticles to improve mucus-penetration and colloidal stability for oral delivery systems. *Curr Opin Chem Eng*. Published online 2016. doi:10.1016/j.coche.2015.11.006

71. Xu Q, Ensign LM, Boylan NJ, et al. Impact of Surface Polyethylene Glycol (PEG) Density on Biodegradable Nanoparticle Transport in Mucus ex Vivo and Distribution in Vivo. *ACS Nano*. 2015;9(9):9217-9227. doi:10.1021/acsnano.5b03876

72. Jokerst J V., Lobovkina T, Zare RN, Gambhir SS. Nanoparticle PEGylation for imaging and therapy. *Nanomedicine*. 2011;6(4):715-728. doi:10.2217/nnm.11.19

73. Pardeike J, Hommoss A, Müller RH. Lipid nanoparticles (SLN, NLC) in cosmetic and pharmaceutical dermal products. *Int J Pharm*. Published online 2009. doi:10.1016/j.ijpharm.2008.10.003

74. Patil H, Feng X, Ye X, Majumdar S, Repka MA. Continuous Production of Fenofibrate Solid Lipid Nanoparticles by Hot-Melt Extrusion Technology: a Systematic Study Based on a Quality by Design Approach. *AAPS J*. Published online 2015. doi:10.1208/s12248-014-9674-8

75. Shegokar R, Singh KK, Müller RH. Production & stability of stavudine solid lipid nanoparticles - From lab to industrial scale. *Int J Pharm*. Published online 2011. doi:10.1016/j.ijpharm.2010.08.014

76. Patil H, Kulkarni V, Majumdar S, Repka MA. Continuous manufacturing of solid lipid nanoparticles by hot melt extrusion. *Int J Pharm*. Published online 2014. doi:10.1016/j.ijpharm.2014.05.024

77. Tiwari R V., Patil H, Repka MA. Contribution of hot-melt extrusion technology to advance drug delivery in the 21st century. *Expert Opin Drug Deliv*. 2016;13(3):451-464. doi:10.1517/17425247.2016.1126246

78. Repka MA, Battu SK, Upadhye SB, et al. Pharmaceutical Applications of Hot-Melt Extrusion: Part II. *Drug Dev Ind Pharm*. 2007;33(10):1043-1057. doi:10.1080/03639040701525627

79. Repka MA, Majumdar S, Battu SK, Srirangam R, Upadhye SB. Applications of hot-melt extrusion for drug delivery. *Expert Opin Drug Deliv*. Published online 2008. doi:10.1517/17425240802583421

80. Pardeike J, Weber S, Zarfl HP, Pagitz M, Zimmer A. Itraconazole-loaded nanostructured lipid carriers (NLC) for pulmonary treatment of aspergillosis in falcons. *Eur J Pharm Biopharm*. Published online 2016. doi:10.1016/j.ejpb.2016.07.018

81. USP Monograph. Accessed February 13, 2021. http://usp35.infostar.com.cn/uspnf/pub/data/v35300/usp35nf30s0_m43724.html

82. Yang W, Peters JI, Williams RO. Inhaled nanoparticles-A current review. *Int J Pharm*. 2008;356(1-2):239-247. doi:10.1016/j.ijpharm.2008.02.011

83. Phan HT, Haes AJ. What Does Nanoparticle Stability Mean? *J Phys Chem C*. 2019;123(27):16495-16507. doi:10.1021/acs.jpcc.9b00913

84. Rivolta I, Panariti A, Lettiero B, et al. Cellular uptake of coumarin-6 as a model drug loaded in solid lipid nanoparticles. *J Physiol Pharmacol*. Published online 2011.

85. Olbrich C, Kayser O, Müller RH. Lipase degradation of Dynasan 114 and 116 solid lipid nanoparticles (SLN) - Effect of surfactants, storage time and crystallinity. *Int J Pharm*. Published online 2002. doi:10.1016/S0378-5173(02)00035-2

86. McCallion ONM, Taylor KMG, Thomas M, Taylor AJ. Nebulization of Fluids of Different Physicochemical Properties with Air-Jet and Ultrasonic Nebulizers. *Pharm Res An Off J Am Assoc Pharm Sci*. Published online 1995. doi:10.1023/A:1016205520044

87. Lim WM, Rajinikanth PS, Mallikarjun C, Kang YB. Formulation and delivery of itraconazole to the brain using a nanolipid carrier system. *Int J Nanomedicine*. Published online 2014. doi:10.2147/IJN.S57565

88. Parikh T, Sandhu HK, Talele TT, Serajuddin ATM. Characterization of Solid Dispersion of Itraconazole Prepared by Solubilization in Concentrated Aqueous Solutions of Weak Organic Acids and Drying. *Pharm Res*. Published online 2016. doi:10.1007/s11095-016-1890-8

89. Dailey LA, Schmehl T, Gessler T, et al. Nebulization of biodegradable nanoparticles: Impact of nebulizer technology and nanoparticle characteristics on aerosol features. *J Control Release*. 2003;86(1):131-144. doi:10.1016/S0168-3659(02)00370-X

90. Labiris NR, Dolovich MB. Pulmonary drug delivery. Part I: Physiological factors affecting therapeutic effectiveness of aerosolized medications. *Br J Clin Pharmacol*. 2003;56(6):588-599. doi:10.1046/j.1365-2125.2003.01892.x

91. Itraconazole | C35H38Cl2N8O4 - PubChem. Accessed September 6, 2020. https://pubchem.ncbi.nlm.nih.gov/compound/Itraconazole#section=Melting-Point

92. Alshehri S, Imam SS, Hussain A, et al. Potential of solid dispersions to enhance solubility, bioavailability, and therapeutic efficacy of poorly water-soluble drugs: newer formulation techniques, current marketed scenario and patents. *Drug Deliv*. Published online 2020. doi:10.1080/10717544.2020.1846638

93. Gupta S, Kesarla R, Omri A. Formulation Strategies to Improve the Bioavailability of Poorly Absorbed Drugs with Special Emphasis on Self-Emulsifying Systems. *ISRN Pharm*. Published online 2013. doi:10.1155/2013/848043

94. Kanuganti S, Jukanti R, Veerareddy PR, Bandari S. Paliperidone-loaded self-emulsifying drug delivery systems (SEDDS) for improved oral delivery. *J Dispers Sci Technol*. Published online 2012. doi:10.1080/01932691.2011.574920

95. Constantinides PP. Lipid Microemulsions for Improving Drug Dissolution and Oral Absorption: Physical and Biopharmaceutical Aspects. *Pharm Res An Off J Am Assoc Pharm Sci*. Published online 1995. doi:10.1023/A:1016268311867

96. Kallakunta VR, Eedara BB, Jukanti R, Ajmeera RK, Bandari S. A Gelucire 44/14 and labrasol based solid self emulsifying drug delivery system: Formulation and evaluation. *J Pharm Investig*. Published online 2013. doi:10.1007/s40005-013-0060-9

97. Humberstone AJ, Charman WN. Lipid-based vehicles for the oral delivery of poorly water soluble drugs. *Adv Drug Deliv Rev*. Published online 1997. doi:10.1016/S0169-409X(96)00494-2

98. Gursoy RN, Benita S. Self-emulsifying drug delivery systems (SEDDS) for improved oral

delivery of lipophilic drugs. *Biomed Pharmacother*. Published online 2004. doi:10.1016/j.biopha.2004.02.001

99. Elsheikh MA, Elnaggar YSR, Gohar EY, Abdallah OY. Nanoemulsion liquid preconcentrates for raloxifene hydrochloride: Optimization and in vivo appraisal. *Int J Nanomedicine*. Published online 2012. doi:10.2147/IJN.S33186

100. Date AA, Desai N, Dixit R, Nagarsenker M. Self-nanoemulsifying drug delivery systems: Formulation insights, applications and advances. *Nanomedicine*. Published online 2010. doi:10.2217/nnm.10.126

101. Balakrishnan P, Lee BJ, Oh DH, et al. Enhanced oral bioavailability of dexibuprofen by a novel solid Self-emulsifying drug delivery system (SEDDS). *Eur J Pharm Biopharm*. Published online 2009. doi:10.1016/j.ejpb.2009.03.001

102. Inugala S, Eedara BB, Sunkavalli S, et al. Solid self-nanoemulsifying drug delivery system (S-SNEDDS) of darunavir for improved dissolution and oral bioavailability: In vitro and in vivo evaluation. *Eur J Pharm Sci*. Published online 2015. doi:10.1016/j.ejps.2015.03.024

103. Franceschinis E, Voinovich D, Grassi M, et al. Self-emulsifying pellets prepared by wet granulation in high-shear mixer: Influence of formulation variables and preliminary study on the in vitro absorption. In: *International Journal of Pharmaceutics*. ; 2005. doi:10.1016/j.ijpharm.2004.07.046

104. Silva LAD, Almeida SL, Alonso ECP, et al. Preparation of a solid self-microemulsifying drug delivery system by hot-melt extrusion. *Int J Pharm*. Published online 2018. doi:10.1016/j.ijpharm.2018.02.020

105. Repka MA, Bandari S, Kallakunta VR, et al. Melt extrusion with poorly soluble drugs – An integrated review. *Int J Pharm*. 2018;535(1-2):68-85. doi:10.1016/j.ijpharm.2017.10.056

106. Shadambikar G, Marathe S, Ji N, et al. Formulation development of itraconazole PEGylated nano-lipid carriers for pulmonary aspergillosis using hot-melt extrusion technology. *Int J Pharm X*. Published online 2021. doi:10.1016/j.ijpx.2021.100074

107. Crowley MM, Zhang F, Repka MA, et al. Pharmaceutical Applications of Hot-Melt Extrusion: Part I. *Drug Dev Ind Pharm*. 2007;33(9):909-926. doi:10.1080/03639040701498759

108. Patil H, Tiwari R V, Repka MA. Hot-Melt Extrusion: from Theory to Application in Pharmaceutical Formulation. *AAPS PharmSciTech*. 2016;17(1):20-42. doi:10.1208/s12249-015-0360-7

109. Kallakunta VR, Sarabu S, Bandari S, Tiwari R, Patil H, Repka MA. An update on the contribution of hot-melt extrusion technology to novel drug delivery in the twenty-first century: part I. *Expert Opin Drug Deliv*. Published online 2019. doi:10.1080/17425247.2019.1609448

110. Shadambikar G, Kipping T, Di-Gallo N, et al. Vacuum compression molding as a screening tool to investigate carrier suitability for hot-melt extrusion formulations. *Pharmaceutics*. Published online 2020. doi:10.3390/pharmaceutics12111019

111. Bookwala M, Thipsay P, Ross S, Zhang F, Bandari S, Repka MA. Preparation of a crystalline salt of indomethacin and tromethamine by hot melt extrusion technology. *Eur J Pharm Biopharm*. Published online 2018. doi:10.1016/j.ejpb.2018.08.001

112. Prasad D, Chauhan H, Atef E. Studying the effect of lipid chain length on the precipitation of a poorly water soluble drug from self-emulsifying drug delivery system on dispersion into aqueous medium. *J Pharm Pharmacol*. Published online 2013. doi:10.1111/jphp.12077

VITA

Gauri Deepak Shadambikar was born on July 14th, 1994, in Mumbai, Maharashtra, India. She received her Bachelor of Pharmacy in 2016 from SNDT Women's University, India. Gauri joined Department of Pharmaceutics and Drug Delivery, at University of Mississippi in Fall of 2016. She published three research articles in peer reviewed journal as a first author and three research papers as a secondary author. She completed her internship at Merck, Darmstadt, Germany in summer of 2018 after completing her Master's in Pharmaceutical Sciences with emphasis in Pharmaceutics and Drug Delivery.

In Fall of 2018 she started her Ph.D. research in hot-melt extrusion technology under the supervision of Dr. Michael Repka. Gauri was inducted into Rho Chi Honor Society in 2019 and was selected as Graduate School Student Ambassador in 2019.